

Low-dimensional Bose gases

U. Al Khawaja¹, J.O. Andersen¹, N.P. Proukakis^{1,2}, and H.T.C. Stoof¹

¹*Institute for Theoretical Physics,*

Utrecht University, Leuvenlaan 4, 3584 CE Utrecht, The Netherlands

²*Foundation for Research and Technology Hellas,*

Institute of Electronic Structure and Laser, P.O. Box 1527, Heraklion 71 110, Crete, Greece

(October 26, 2018)

We present an improved many-body T-matrix theory for partially Bose-Einstein condensed atomic gases by treating the phase fluctuations exactly. The resulting mean-field theory is valid in arbitrary dimensions and able to describe the low-temperature crossover between three, two and one-dimensional Bose gases. When applied to a degenerate two-dimensional atomic hydrogen gas, we obtain a reduction of the three-body recombination rate which compares favorably with experiment. Supplementing the mean-field theory with a renormalization-group approach to treat the critical fluctuations, we also incorporate into the theory the Kosterlitz-Thouless transition that occurs in a homogeneous Bose gas in two dimensions. In particular, we calculate the critical conditions for the Kosterlitz-Thouless phase transition as a function of the microscopic parameters of the theory. The proposed theory is further applied to a trapped one-dimensional Bose gas, where we find good agreement with exact numerical results obtained by solving a nonlinear Langevin field equation.

PACS numbers: 03.75.Fi, 67.40.-w, 32.80.Pj

I. INTRODUCTION

Low-dimensional Bose gases have recently attracted attention both experimentally and theoretically. The interest in these systems stems from the fact that the physics of low-dimensional systems is fundamentally different from the physics of systems in three dimensions. One and two-dimensional Bose-Einstein condensates have recently been created in the experiment of Görlitz *et al.* [1]. This was achieved by lowering the mean-field interaction energy in a three-dimensional condensate below the energy splitting of either one or two of the directions of the harmonic trap, to obtain a two-dimensional or one-dimensional condensate, respectively. In a number of other experiments a one-dimensional Bose-Einstein condensate was also created in a ⁶Li-⁷Li mixture [2] and on a microchip [3,4].

Theoretically, low-dimensional Bose gases are particularly interesting due to the enhanced importance of phase fluctuations [5–8]. Because of these fluctuations, Bose-Einstein condensation cannot take place in a homogeneous one-dimensional Bose gas at all temperatures and in a homogeneous two-dimensional Bose gas at any nonzero temperature. This is formalized in the Mermin-Wagner-Hohenberg theorem [9,10]. Since this theorem is valid only in the thermodynamic limit, it does not apply to trapped Bose gases. Therefore, the question arises whether under certain conditions we are dealing with a true condensate, where the phase is coherent over a distance of the order of the size of the system, or only with a so-called “quasicondensate” [11], where the phase is coherent over a distance less than the size of the system [5–8]. This is one of the main questions, which we

address quantitatively in this paper.

In the successful Popov theory for three-dimensional partially Bose-Einstein condensed gases, the phase fluctuations are taken into account up to the second order around the mean field. In view of the above-mentioned importance of phase fluctuations in lower dimensions, this is insufficient in general and leads to infrared divergences. In previous work by three of us, the phase fluctuations were taken into account exactly [12]. The result is a mean-field theory which is free of the infrared divergences in all dimensions. In the present paper, we first review this modified Popov theory and then extend it to the many-body T-matrix theory, by including the effect of the medium on the scattering properties of the atoms in the gas. The present approach improves on previous attempts by Petrov *et al.* [7,8] to describe low-dimensional Bose gases by explicitly incorporating also the effect of density fluctuations into the theory. As a result both quantum and thermal depletion of the (quasi)condensate can now be accounted for and the theory is no longer only valid at very low temperatures where the depletion, and therefore the thermal component in the gas, is negligible. Most importantly, we present an equation of state for the low-dimensional Bose gas that is free of infrared divergences and thus valid in any dimension. For a trapped Bose gas this implies that we can determine, for a given number of atoms, the density profile of both the (quasi)condensate and the thermal cloud in the gas for any aspect ratio of the trap. Also the interesting crossover problem from a three-dimensional Bose gas to a one or two-dimensional one, that is presently being explored experimentally [1], can be addressed as well.

In the present paper we first use the modified many-

body T-matrix theory to calculate the one-particle density matrix and determine its off-diagonal long-range order. We also calculate the fractional depletion of the (quasi)condensate at zero temperature in one, two, and three dimensions. Next, we study the two-dimensional homogeneous Bose gas in considerable detail. After having included the phase fluctuations due to vortex pairs by a renormalization group approach, we apply the modified many-body T-matrix theory to perform an *ab initio* study of the Kosterlitz-Thouless phase transition [13] from the superfluid to the normal state. Since this is a topological phase transition, it cannot be described within mean-field theory. Therefore, we proceed as follows. We first use the modified many-body T-matrix theory to calculate the quasicondensate density and the fugacity of vortices. These results are then used as initial conditions for a Kosterlitz renormalization group calculation. In this manner, we are incorporating critical fluctuations and able to calculate nonuniversal quantities such as the critical temperature for the Kosterlitz-Thouless phase transition as a function of the density and the microscopic parameters of the theory.

Finally, we apply the theory to a trapped one-dimensional Bose gas, where we calculate the density profile at different temperatures. From this we extract the crossover temperature for the appearance of a (quasi)condensate as a function of the interaction strength. We also calculate the behavior of the phase correlation function which determines whether there exists a true condensate or only a quasicondensate. These predictions are compared to exact results based on a stochastic nonlinear field equation for the Bose gas [14].

The paper is organized as follows. In Sec. II, we present and discuss the Popov theory and its infrared problems. We also present our modified mean-field theory in the homogeneous limit. In Sec. III, we compare the latter with exact results in one dimension, and with results obtained in the Popov approximation in two and three dimensions. We also calculate the reduction of the three-body recombination rate for a two-dimensional hydrogen gas and compare it to the experiment of Safonov *et al.* [15]. In Sec. IV, we study the Kosterlitz-Thouless phase transition and in Sec. V, we generalize the many-body T-matrix theory to inhomogeneous situations. In particular, we consider then a one-dimensional trapped Bose gas, for which we compare our predictions to numerically exact results. Finally, we conclude and summarize in Sec. VI.

II. MODIFIED POPOV THEORY

In this section, we derive the modified Popov theory by treating the phase fluctuations exactly. We also discuss how to incorporate many-body effects into the theory. Finally, we give additional arguments for the correctness

of our approach by using an effective action for the density and phase dynamics in a superfluid system that is known to give exact results in the long-wavelength limit.

A. Phase fluctuations

In order to explain the infrared problems associated with the phase fluctuations of the condensate most clearly, we first treat a homogeneous Bose gas in a box of volume V . Later we generalize to the inhomogeneous case. The starting point is the grand-canonical Hamiltonian in second-quantized language

$$H = \int d\mathbf{x} \hat{\psi}^\dagger(\mathbf{x}) \left[-\frac{\hbar^2}{2m} \nabla^2 - \mu \right] \hat{\psi}(\mathbf{x}) + \frac{1}{2} \int d\mathbf{x} \int d\mathbf{x}' \hat{\psi}^\dagger(\mathbf{x}) \hat{\psi}^\dagger(\mathbf{x}') \times V(\mathbf{x} - \mathbf{x}') \hat{\psi}(\mathbf{x}') \hat{\psi}(\mathbf{x}), \quad (1)$$

where μ is the chemical potential, and $V(\mathbf{x})$ is the atomic two-body interaction potential. The mass of the atoms is denoted by m , and $\hat{\psi}^\dagger(\mathbf{x})$ and $\hat{\psi}(\mathbf{x})$ are the usual creation and annihilation field operators, respectively.

In the Bose systems considered here and those realized in experiment, the temperatures are so low that only s -wave scattering is important. Consequently, it is convenient to neglect the momentum dependence of the interatomic interaction and use $V(\mathbf{x} - \mathbf{x}') = V_0 \delta(\mathbf{x} - \mathbf{x}')$. In principle this leads to ultraviolet divergences, but these can easily be dealt with, as we show later on. The Hamiltonian then reduces to

$$H = \int d\mathbf{x} \hat{\psi}^\dagger(\mathbf{x}) \left[-\frac{\hbar^2}{2m} \nabla^2 - \mu \right] \hat{\psi}(\mathbf{x}) + \frac{1}{2} \int d\mathbf{x} V_0 \hat{\psi}^\dagger(\mathbf{x}) \hat{\psi}^\dagger(\mathbf{x}) \hat{\psi}(\mathbf{x}) \hat{\psi}(\mathbf{x}). \quad (2)$$

In the presence of a Bose-Einstein condensate the annihilation operator is parametrized as

$$\hat{\psi}(\mathbf{x}) = \sqrt{n_0} + \hat{\psi}'(\mathbf{x}), \quad (3)$$

where n_0 is the condensate density and $\hat{\psi}'(\mathbf{x})$ describes the fluctuations. The standard one-loop expressions for the density n and the chemical potential μ are obtained after a quadratic approximation to the Hamiltonian in Eq. (2), i.e., by neglecting terms that are of third and fourth order in the fluctuations. This yields [11,16]

$$n = n_0 + \frac{1}{V} \sum_{\mathbf{k}} \left[\frac{\epsilon_{\mathbf{k}} + n_0 V_0 - \hbar \omega_{\mathbf{k}}}{2 \hbar \omega_{\mathbf{k}}} + \frac{\epsilon_{\mathbf{k}} + n_0 V_0}{\hbar \omega_{\mathbf{k}}} N(\hbar \omega_{\mathbf{k}}) \right], \quad (4)$$

$$\frac{\mu}{V_0} = n_0 + \frac{1}{V} \sum_{\mathbf{k}} \left[\frac{2\epsilon_{\mathbf{k}} + n_0 V_0 - 2\hbar\omega_{\mathbf{k}}}{2\hbar\omega_{\mathbf{k}}} + \frac{2\epsilon_{\mathbf{k}} + n_0 V_0}{\hbar\omega_{\mathbf{k}}} N(\hbar\omega_{\mathbf{k}}) \right], \quad (5)$$

where $\hbar\omega_{\mathbf{k}} = (\epsilon_{\mathbf{k}}^2 + 2n_0 V_0 \epsilon_{\mathbf{k}})^{1/2}$ is the Bogoliubov dispersion relation, $N(x) = 1/(e^{\beta x} - 1)$ is the Bose-Einstein distribution function, and $\beta = 1/k_B T$ is the inverse thermal energy.

In agreement with the Mermin-Wagner-Hohenberg theorem, the momentum sums in Eqs. (4) and (5) contain terms that are infrared divergent at all temperatures in one dimension and at any nonzero temperature in two dimensions. The physical reason for these “dangerous” terms is that the above expressions have been derived by taking into account only quadratic fluctuations around the classical result n_0 , i.e., by writing the annihilation operator for the atoms as $\hat{\psi}(\mathbf{x}) = \sqrt{n_0} + \hat{\psi}'(\mathbf{x})$ and neglecting in the Hamiltonian terms of third and fourth order in $\hat{\psi}'(\mathbf{x})$. As a result the phase fluctuations of the condensate give the quadratic contribution $n_0 \langle \hat{\chi}(\mathbf{x}) \hat{\chi}(\mathbf{x}) \rangle$ to the right-hand side of the above equations, whereas an exact approach that sums up all the higher-order terms in the expansion would clearly give no contribution at all to these local quantities because $n_0 \langle e^{-i\hat{\chi}(\mathbf{x})} e^{i\hat{\chi}(\mathbf{x})} \rangle = n_0 (1 + \langle \hat{\chi}(\mathbf{x}) \hat{\chi}(\mathbf{x}) \rangle + \dots) = 1$. To correct for this we thus need to subtract the quadratic contribution of the phase fluctuations, which from Eqs. (4) and (5) is seen to be given by

$$n_0 \langle \hat{\chi}(\mathbf{x}) \hat{\chi}(\mathbf{x}) \rangle = \frac{1}{V} \sum_{\mathbf{k}} \frac{n_0 V_0}{2\hbar\omega_{\mathbf{k}}} [1 + 2N(\hbar\omega_{\mathbf{k}})]. \quad (6)$$

As expected, the infrared divergences that occur in the one and two-dimensional cases are removed by performing this subtraction.

After having removed the spurious contributions from the phase fluctuations of the condensate, the resulting expressions turn out to be ultraviolet divergent. These divergences are removed by the standard renormalization of the bare coupling constant V_0 . Apart from a subtraction, this essentially amounts to replacing everywhere the bare two-body potential V_0 by the two-body T-matrix evaluated at zero initial and final relative momenta and at the energy -2μ , which we denote from now on by $T^{2B}(-2\mu)$. It is formally defined by

$$\frac{1}{T^{2B}(-2\mu)} = \frac{1}{V_0} + \frac{1}{V} \sum_{\mathbf{k}} \frac{1}{2\epsilon_{\mathbf{k}} + 2\mu}. \quad (7)$$

Note that the energy argument of the T-matrix is -2μ , because this is precisely the energy it costs to excite two atoms from the condensate [17,18]. After renormalization, the density and chemical potential are

$$n = n_0 + \frac{1}{V} \sum_{\mathbf{k}} \left[\frac{\epsilon_{\mathbf{k}} - \hbar\omega_{\mathbf{k}}}{2\hbar\omega_{\mathbf{k}}} + \frac{n_0 T^{2B}(-2\mu)}{2\epsilon_{\mathbf{k}} + 2\mu} + \frac{\epsilon_{\mathbf{k}}}{\hbar\omega_{\mathbf{k}}} N(\hbar\omega_{\mathbf{k}}) \right], \quad (8)$$

$$\begin{aligned} \mu &= (2n - n_0) T^{2B}(-2\mu) \\ &= (2n' + n_0) T^{2B}(-2\mu), \end{aligned} \quad (9)$$

where $n' = n - n_0$ represents the depletion of the condensate due to quantum and thermal fluctuations and the Bogoliubov quasiparticle dispersion now equals $\hbar\omega_{\mathbf{k}} = [\epsilon_{\mathbf{k}}^2 + 2n_0 T^{2B}(-2\mu) \epsilon_{\mathbf{k}}]^{1/2}$. The most important feature of Eqs. (8) and (9) is that they contain no infrared and ultraviolet divergences and therefore can be applied in any dimension and at all temperatures, even if no condensate exists.

Note that Eq. (6) is also ultraviolet divergent. The ultraviolet divergences are removed by the same renormalization of the bare interaction V_0 and the final result is

$$\begin{aligned} \langle \hat{\chi}(\mathbf{x}) \hat{\chi}(\mathbf{x}) \rangle &= \frac{T^{2B}(-2\mu)}{V} \sum_{\mathbf{k}} \left[\frac{1}{2\hbar\omega_{\mathbf{k}}} [1 + 2N(\hbar\omega_{\mathbf{k}})] \right. \\ &\quad \left. - \frac{1}{2\epsilon_{\mathbf{k}} + 2\mu} \right]. \end{aligned} \quad (10)$$

We will return to the physics of this important expression in Sec. II C below.

B. Many-body T-matrix

In the previous section, we presented the modified Popov theory that takes the phase fluctuations into account exactly. The final results in Eqs. (8), (9), and (10) involve the two-body T-matrix. The two-body T-matrix takes into account successive two-body scattering processes in vacuum. However, it neglects the many-body effects of the surrounding gas. In order to take this into account as well, we must use the many-body T-matrix instead of the two-body T-matrix in Eqs. (8), (9) and (10). Many-body effects have been shown to be appreciable in three dimensions only very close to the transition temperature [19], but turn out to be much more important in one and two dimensions [16]. Since the effects of the medium on the scattering properties of the atoms is only important at relatively high temperatures, we can apply a Hartree-Fock approximation to obtain for the many-body T-matrix

$$\begin{aligned} T^{\text{MB}}(-2\mu) &= T^{2B}(-2\mu) \\ &\times \left[1 + T^{2B}(-2\mu) \frac{1}{V} \sum_{\mathbf{k}} \frac{N(\epsilon_{\mathbf{k}} + n_0 T^{\text{MB}}(-2\mu))}{\epsilon_{\mathbf{k}} + \mu} \right]^{-1}. \end{aligned} \quad (11)$$

The situation is in fact slightly more complicated because we actually have two coupling constants in the equation for the chemical potential, which is the homogeneous version of the Gross-Pitaevskii equation. When two atoms in the condensate collide at zero momentum, they both require an energy μ to be excited from the condensate, and thus the coupling is evaluated at -2μ . This is the coupling that multiplies n_0 in the Gross-Pitaevskii equation. On the other hand, the coupling that multiplies n' in the Gross-Pitaevskii equation involves one condensate atom and one atom in the thermal cloud, so that this coupling should now be evaluated at $-\mu$. The equation for the chemical potential thus becomes

$$\mu = 2n'T^{\text{MB}}(-\mu) + n_0T^{\text{MB}}(-2\mu). \quad (12)$$

Note that the existence of two different many-body coupling constants for the interatomic interactions has previously been discussed by Proukakis *et al.* [20]. (See however also Ref. [21].) This lead these authors to the so-called *G1*-theory, which is qualitatively somewhat similar to Eq. (12) but differs in detail.

C. Long-wavelength physics

We have given physical arguments for how to identify and subtract the contribution to Eqs. (4) and (5) from the phase fluctuations of the condensate. At this point, we would like to give a somewhat more rigorous field-theoretical argument. The Euclidean action that corresponds to the Hamiltonian in Eq. (2) is

$$S[\psi^*, \psi] = \int_0^{\hbar\beta} d\tau \int d\mathbf{x} \psi^* \left[\hbar \frac{\partial}{\partial \tau} - \frac{\hbar^2}{2m} \nabla^2 - \mu \right] \psi - \frac{1}{2} \int_0^{\hbar\beta} d\tau \int d\mathbf{x} V_0 |\psi|^4. \quad (13)$$

If we substitute $\psi(\mathbf{x}, \tau) = \sqrt{n + \delta n(\mathbf{x}, \tau)} e^{i\chi(\mathbf{x}, \tau)}$ into Eq. (13), we obtain the action

$$S[\delta n, \chi] = \int_0^{\hbar\beta} d\tau \int d\mathbf{x} \left[\frac{1}{2} \hbar \frac{\partial \delta n}{\partial \tau} + i\hbar(n + \delta n) \frac{\partial \chi}{\partial \tau} + \frac{\hbar^2}{2m} n (\nabla \chi)^2 + \frac{1}{2} \delta n \left(\frac{\hbar^2}{2mn} \nabla^2 + V_0 \right) \delta n \right]. \quad (14)$$

Here, n is the average total density of the gas and $\delta n(\mathbf{x}, \tau)$ represents the fluctuations. At zero temperature, this action is exact in the long-wavelength limit, if $(\hbar^2 k^2 / 2mn + V_0)$ is replaced by $\chi_{nn}^{-1}(\mathbf{k})$, where $\chi_{nn}(\mathbf{k})$ is the exact static density-density correlation function.

By using the classical equation of motion to eliminate the phase $\chi(\mathbf{x}, \tau)$, we obtain the following action for the density fluctuations $\delta n(\mathbf{x}, \tau)$:

$$S[\delta n] = \int_0^{\hbar\beta} d\tau \int d\mathbf{x} \left[-\frac{m}{n} \frac{\partial \delta n}{\partial \tau} \nabla^{-2} \frac{\partial \delta n}{\partial \tau} + \frac{1}{2} \delta n \chi_{nn}^{-1}(-i\nabla) \delta n \right]. \quad (15)$$

The density fluctuations are therefore determined by

$$\langle \delta \hat{n}(\mathbf{x}) \delta \hat{n}(\mathbf{x}') \rangle = \frac{1}{V} \sum_{\omega_n, \mathbf{k}} \frac{n \epsilon_{\mathbf{k}}}{\beta} \left[\frac{1}{(\hbar \omega_n)^2 + (\hbar \omega_{\mathbf{k}})^2} \right] \times e^{i\mathbf{k} \cdot (\mathbf{x} - \mathbf{x}')}, \quad (16)$$

where $\omega_n = 2\pi n / \hbar \beta$ are the even Matsubara frequencies and $\hbar \omega_{\mathbf{k}} = \sqrt{n \epsilon_{\mathbf{k}} / \chi_{nn}(\mathbf{k})}$. Summing over these Matsubara frequencies, we obtain

$$\langle \delta \hat{n}(\mathbf{x}) \delta \hat{n}(\mathbf{x}') \rangle = \frac{1}{V} \sum_{\mathbf{k}} \frac{n \epsilon_{\mathbf{k}}}{\hbar \omega_{\mathbf{k}}} [1 + 2N(\hbar \omega_{\mathbf{k}})] \times e^{i\mathbf{k} \cdot (\mathbf{x} - \mathbf{x}')}. \quad (17)$$

Similarly, by using the classical equation of motion for $\delta n(\mathbf{x}, \tau)$, we obtain from Eq. (14) the following action for the phase fluctuations:

$$S[\chi] = \int_0^{\hbar\beta} d\tau \int d\mathbf{x} \left[\hbar^2 \frac{\partial \chi}{\partial \tau} \chi_{nn}(-i\nabla) \frac{\partial \chi}{\partial \tau} + \frac{\hbar^2 n}{2m} (\nabla \chi)^2 \right]. \quad (18)$$

From this action, it is straightforward to calculate the propagator for the field $\chi(\mathbf{x}, \tau)$ and thereby the correlation function $\langle \hat{\chi}(\mathbf{x}) \hat{\chi}(\mathbf{x}') \rangle$. The result is

$$\langle \hat{\chi}(\mathbf{x}) \hat{\chi}(\mathbf{x}') \rangle = \frac{1}{V} \sum_{\mathbf{k}} \frac{1}{\chi_{nn}(\mathbf{k})} \frac{1}{2\hbar \omega_{\mathbf{k}}} [1 + 2N(\hbar \omega_{\mathbf{k}})] \times e^{i\mathbf{k} \cdot (\mathbf{x} - \mathbf{x}')}. \quad (19)$$

Setting $\mathbf{x}' = \mathbf{x}$, we recover Eq. (10) in the long-wavelength limit, if we use $\chi_{nn}(\mathbf{k}) \simeq 1/T^{\text{MB}}(-2\mu)$ for the static density-density correlation function in that limit. It is important to mention that Eq. (19) is often used for the short-wavelength part of the phase fluctuations as well [7,8]. This is, however, incorrect because it contains ultraviolet divergences due to the fact that the above procedure neglects interaction terms between density and phase fluctuations that are only irrelevant at large wavelengths. The correct short wavelength behavior is given in Eq. (10).

III. COMPARISON WITH POPOV THEORY

We proceed to compare predictions based on Eqs. (8), (9), and (10) with exact results in one dimension and results based on the Popov theory in two and three dimensions. We consider only the homogeneous case here and discuss the inhomogeneous Bose gas in Sec. V

A. One dimension

To understand the physical meaning of the quantity n_0 in Eqs. (8) and (9), i.e., whether it is the quasicondensate density or the true condensate density, we must determine the off-diagonal long-range behavior of the one-particle density matrix. Because this is a nonlocal property of the Bose gas, the phase fluctuations contribute and we find in the large- $|\mathbf{x}|$ limit

$$\begin{aligned} \langle \hat{\psi}^\dagger(\mathbf{x}) \hat{\psi}(\mathbf{0}) \rangle &\simeq n_0 \langle e^{-i(\hat{\chi}(\mathbf{x}) - \hat{\chi}(\mathbf{0}))} \rangle \\ &= n_0 e^{-\frac{1}{2} \langle [\hat{\chi}(\mathbf{x}) - \hat{\chi}(\mathbf{0})]^2 \rangle} . \end{aligned} \quad (20)$$

Using Eq. (10), we obtain for the exponent in Eq. (20)

$$\begin{aligned} \langle [\hat{\chi}(\mathbf{x}) - \hat{\chi}(\mathbf{0})]^2 \rangle &= \frac{T^{\text{MB}}(-2\mu)}{V} \sum_{\mathbf{k}} \left[\frac{1}{\hbar\omega_{\mathbf{k}}} [1 + 2N(\hbar\omega_{\mathbf{k}})] \right. \\ &\quad \left. - \frac{1}{\epsilon_{\mathbf{k}} + \mu} \right] \times [1 - \cos(\mathbf{k} \cdot \mathbf{x})] . \end{aligned} \quad (21)$$

Writing the sum over wave vectors \mathbf{k} as an integral, the phase fluctuations at zero temperature can be written as

$$\langle [\hat{\chi}(\mathbf{x}) - \hat{\chi}(\mathbf{0})]^2 \rangle = \frac{1}{2\pi n_0 \xi} \int_0^\infty dk \frac{1 - \cos(kx)}{k\sqrt{k^2 + 1}} , \quad (22)$$

where $\xi = \hbar/[4mn_0 T^{2\text{B}}(-2\mu)]^{1/2}$ is the correlation length. Note that we have used that $T^{\text{MB}}(-2\mu) = T^{2\text{B}}(-2\mu)$ at zero temperature and that the chemical potential, as we show shortly, is to a good approximation equal to $n_0 T^{2\text{B}}(-2\mu)$. The integration can be performed analytically and the result is

$$\begin{aligned} \langle [\hat{\chi}(\mathbf{x}) - \hat{\chi}(\mathbf{0})]^2 \rangle &= \frac{1}{2\pi n_0 \xi} \left[\frac{\pi x}{2\xi} {}_1F_2(1/2; 1, 3/2; x^2/4\xi^2) \right. \\ &\quad \left. - \frac{x^2}{2\xi^2} {}_2F_3(1, 1; 3/2, 3/2; 2x^2/4\xi^2) \right] , \end{aligned} \quad (23)$$

where ${}_iF_j(\alpha_1, \alpha_2, \dots, \alpha_i; \beta_1, \beta_2, \dots, \beta_j; x)$ are hypergeometric functions. In the limit $|\mathbf{x}| \rightarrow \infty$, Eq. (23) reduces to

$$\langle [\hat{\chi}(\mathbf{x}) - \hat{\chi}(\mathbf{0})]^2 \rangle \simeq \frac{1}{2\pi n_0 \xi} \log(x/\xi) . \quad (24)$$

Using Eq. (24) we find that the one-particle density matrix behaves for $|\mathbf{x}| \rightarrow \infty$ as

$$\langle \hat{\psi}^\dagger(\mathbf{x}) \hat{\psi}(\mathbf{0}) \rangle \simeq \frac{n_0}{(x/\xi)^{1/4\pi n_0 \xi}} . \quad (25)$$

A few remarks are in order. First, the asymptotic behavior of the one-particle density matrix at zero temperature proves that the gas is not Bose-Einstein condensed and that n_0 should be identified with the quasicondensate density. Second, in the weakly-interacting limit

$4\pi n \xi \gg 1$ the depletion is small, so that, to first approximation, we can use $n_0 \simeq n$ in the exponent $\eta = 1/4\pi n_0 \xi$. Indeed, from Eqs. (8) and (9) we obtain the following expression for the fractional depletion of the quasicondensate

$$\frac{n - n_0}{n} = \frac{1}{4\pi n \xi} \left(\frac{\sqrt{2}}{4} \pi - 1 \right) . \quad (26)$$

We see that the expansion parameter is $1/4\pi n \xi$ and, therefore, that the depletion is very small. Keeping this in mind, Eq. (25) is in complete agreement with the exact result obtained by Haldane [22]. Note that our theory cannot describe the strongly-interacting case $4\pi n \xi \ll 1$, where the one-dimensional Bose gas behaves as a Tonks gas [23,24].

Finally, our results show that at a nonzero temperature the phase fluctuations increase as $\langle [\hat{\chi}(\mathbf{x}) - \hat{\chi}(\mathbf{0})]^2 \rangle \propto |\mathbf{x}|$ for large distances, and thus that the off-diagonal one-particle density matrix vanishes exponentially. Hence, at nonzero temperatures not even a quasicondensate exists and we have to use the equation of state for the normal state to describe the gas, i.e.,

$$n = \frac{1}{V} \sum_{\mathbf{k}} N(\epsilon_{\mathbf{k}} + \hbar\Sigma - \mu) , \quad (27)$$

where the Hartree-Fock self-energy satisfies

$$\hbar\Sigma = 2n T^{\text{MB}}(-\hbar\Sigma) , \quad (28)$$

and the many-body T-matrix obeys

$$\begin{aligned} T^{\text{MB}}(-\hbar\Sigma) &= T^{2\text{B}}(-\hbar\Sigma) \\ &\times \left[1 + T^{2\text{B}}(-\hbar\Sigma) \frac{1}{V} \sum_{\mathbf{k}} \frac{N(\epsilon_{\mathbf{k}} + \hbar\Sigma - \mu)}{\epsilon_{\mathbf{k}} + \hbar\Sigma/2} \right]^{-1} , \end{aligned} \quad (29)$$

Note that the last three equations for the description of the normal phase of the Bose gas are again valid for an arbitrary number of dimensions.

B. Two dimensions

In analogy with Eq. (22), we obtain for the phase fluctuations in two dimensions at zero temperature

$$\langle [\hat{\chi}(\mathbf{x}) - \hat{\chi}(\mathbf{0})]^2 \rangle = \frac{1}{2\pi^2 n_0 \xi} \int_0^\infty dk \frac{1 - \cos(kx)}{\sqrt{k^2 + 1}} , \quad (30)$$

Therefore we now find in the limit $|\mathbf{x}| \rightarrow \infty$ that

$$\langle \hat{\psi}^\dagger(\mathbf{x}) \hat{\psi}(\mathbf{0}) \rangle = n_0 \quad (31)$$

and n_0 is clearly the condensate density of the gas. However, at nonzero temperatures the correlation function behaves as

$$\langle \hat{\psi}^\dagger(\mathbf{x})\hat{\psi}(0) \rangle \simeq \frac{n_0}{(x/\xi)^{1/n_0\Lambda^2}}, \quad (32)$$

where $\Lambda = \sqrt{2\pi\hbar^2/mk_B T}$ is the thermal de Broglie wavelength and n_0 corresponds again to the quasicondensate density. At zero temperature, the fractional depletion of the condensate in the Popov approximation was first calculated by Schick [17]. He obtained

$$\frac{n - n_0}{n} = \frac{1}{4\pi} T^{2B}(-2\mu), \quad (33)$$

where the chemical potential satisfies $\mu = nT^{2B}(-2\mu)$. The corresponding result based on Eqs. (8) and (9) is

$$\frac{n - n_0}{n} = \frac{1}{4\pi} (1 - \ln 2) T^{2B}(-2\mu), \quad (34)$$

where μ now satisfies Eq. (9). In two dimensions, the depletion predicted by the Popov theory is thus too large by a factor of approximately 3.

In a number of applications, we need to calculate many-body correlators. For instance, in order to calculate how a quasicondensate modifies the two-body relaxation constants of a spin-polarized two-dimensional Bose gas, we need to know $K^{(2)}(T) \equiv \langle \hat{\psi}^\dagger(\mathbf{x})\hat{\psi}^\dagger(\mathbf{x})\hat{\psi}(\mathbf{x})\hat{\psi}(\mathbf{x}) \rangle / 2n^2$. This correlator was considered in Ref. [25] using the many-body T-matrix theory with an appropriate cutoff to remove the infrared divergences. An exact treatment of the phase fluctuations leads however directly to an infrared finite result as we show now. Using the parametrization in Eq. (3) for the annihilation operators, we obtain first of all

$$\begin{aligned} \langle \hat{\psi}^\dagger(\mathbf{x})\hat{\psi}^\dagger(\mathbf{x})\hat{\psi}(\mathbf{x})\hat{\psi}(\mathbf{x}) \rangle &= n_0^2 + n_0 \left[\langle \hat{\psi}'(\mathbf{x})\hat{\psi}'(\mathbf{x}) \rangle \right. \\ &\quad \left. + \langle \hat{\psi}'^\dagger(\mathbf{x})\hat{\psi}'^\dagger(\mathbf{x}) \rangle + 4\langle \hat{\psi}'^\dagger(\mathbf{x})\hat{\psi}'(\mathbf{x}) \rangle \right] \\ &\quad + 2\langle \hat{\psi}'^\dagger(\mathbf{x})\hat{\psi}'(\mathbf{x}) \rangle^2 \\ &\quad + \langle \hat{\psi}'(\mathbf{x})\hat{\psi}'(\mathbf{x}) \rangle \langle \hat{\psi}'^\dagger(\mathbf{x})\hat{\psi}'^\dagger(\mathbf{x}) \rangle. \end{aligned} \quad (35)$$

The normal average is given by $\langle \hat{\psi}'^\dagger(\mathbf{x})\hat{\psi}'(\mathbf{x}) \rangle = n' + n_0 \langle \hat{\chi}(\mathbf{x})\hat{\chi}(\mathbf{x}) \rangle$ and the anomalous average obeys $\langle \hat{\psi}'(\mathbf{x})\hat{\psi}'(\mathbf{x}) \rangle = -n_0 \langle \hat{\chi}(\mathbf{x})\hat{\chi}(\mathbf{x}) \rangle$, as we have seen. Using this, Eq. (35) can then be written as

$$\begin{aligned} \langle \hat{\psi}^\dagger(\mathbf{x})\hat{\psi}^\dagger(\mathbf{x})\hat{\psi}(\mathbf{x})\hat{\psi}(\mathbf{x}) \rangle &= n_0^2 [1 + 2\langle \hat{\chi}(\mathbf{x})\hat{\chi}(\mathbf{x}) \rangle \\ &\quad + 3\langle \hat{\chi}(\mathbf{x})\hat{\chi}(\mathbf{x}) \rangle^2] \\ &\quad + 4n_0 [1 + \langle \hat{\chi}(\mathbf{x})\hat{\chi}(\mathbf{x}) \rangle] n' + 2(n')^2. \end{aligned} \quad (36)$$

Writing the correlator in this form, we explicitly see that the infrared divergences are due to spurious contributions from the phase fluctuations. Removing them, we obtain for the renormalized correlator

$$K_R^{(2)}(T) = \frac{1}{2n^2} [n_0^2 + 4n_0 n' + 2(n')^2]. \quad (37)$$

We would like to point out that critical fluctuations are not treated within our mean-field theory. This is of course essential in the study of the Kosterlitz-Thouless phase transition and we return to this issue in Sec. IV. However, an example of a physical observable where phase fluctuations are not important, is the three-body recombination rate constant. We are at this point, therefore, already in the position to determine the reduction of the three-body recombination rate constant due to the presence of a quasicondensate. This can be expressed as [25]

$$\frac{L^N}{L(T)} \simeq \left\{ \left[\frac{T^{2B}(-2\mu)}{T^{2B}(-2\hbar\Sigma)} \right]^6 K_R^{(3)}(T) \right\}^{-1}, \quad (38)$$

where L^N is the recombination rate constant in the normal phase, which is essentially independent of temperature, and the self-energy satisfies $\hbar\Sigma = 2nT^{2B}(-\hbar\Sigma)$. The renormalized three-body correlator

$$K_R^{(3)}(T) = \frac{1}{6n^3} [n_0^3 + 9n_0^2 n' + 18n_0 (n')^2 + 6(n')^3] \quad (39)$$

is obtained from the expression for the correlation function $\langle \hat{\psi}^\dagger(\mathbf{x})\hat{\psi}^\dagger(\mathbf{x})\hat{\psi}^\dagger(\mathbf{x})\hat{\psi}(\mathbf{x})\hat{\psi}(\mathbf{x})\hat{\psi}(\mathbf{x}) \rangle$ by removing, as before, the spurious contributions from the phase fluctuations. Moreover, in two dimensions the T-matrix depends logarithmically on the chemical potential as

$$T^{2B}(-2\mu) = \frac{4\pi\hbar^2}{m} \frac{1}{\ln(2\hbar^2/\mu a^2)}, \quad (40)$$

where a is the two-dimensional s -wave scattering length. In the case of atomic hydrogen adsorbed on a superfluid helium film, the scattering length was found to be $a = 2.4a_0$ [26], where a_0 is the Bohr radius. However, there is some uncertainty in this number because the hydrogen wave function perpendicular to the helium surface is not known very accurately. In order to compare with experiment, we may therefore allow a to vary somewhat.

In Fig. 1, we show the reduction of the three-body recombination rate as a function of the density at a fixed temperature $T = 190$ mK for three different values of a . As can clearly be seen from Fig. 1, the reduction of the three-body recombination rate is very sensitive to the value of a . What is most important at this point is that at high densities our calculation shows that the reduction of the recombination rate is much larger than the factor of 6 predicted by Kagan *et al.* [27]. Such large reduction rates are indeed observed experimentally [15]. A direct comparison, however, between the results of our theory and the measurements of Safonov *et al.* cannot be made here, since the density and temperature of the adsorbed hydrogen gas were not measured directly, but inferred from the properties of the three-dimensional buffer gas. Because this procedure requires knowledge of the equation of state

of the two-dimensional Bose gas absorbed on the superfluid helium film, the raw experimental data needs to be reanalyzed with the theory presented in this paper. We can, however, compare the density at which the recombination rate starts to deviate considerably from the result in the normal state. For the temperature of $T = 190$ mK, where most of the experimental data is taken, this is at a density of about $1.0 \times 10^{13} \text{ cm}^{-2}$, which is in excellent agreement with experiment. In view of this and the above mentioned problems we thus conclude that our results present a compelling theoretical explanation of the experimental findings.

C. Three dimensions

The Popov theory has been very successful in describing the properties of dilute three-dimensional trapped Bose gases. It is therefore important to check that an exact treatment of the phase fluctuations leads at most to small changes in the predictions for the three-dimensional case.

At zero temperature, the fractional depletion within the Popov theory was first calculated by Lee and Yang [28] and is given by

$$\frac{n - n_0}{n} = \frac{8}{3} \sqrt{\frac{na^3}{\pi}}, \quad (41)$$

where a is the s -wave scattering length and we have used

$$T^{2B}(-2\mu) = \frac{4\pi a \hbar^2}{m}. \quad (42)$$

The result that follows from Eqs. (8) and (9) is

$$\frac{n - n_0}{n} = \left(\frac{32}{3} - 2\sqrt{2\pi} \right) \sqrt{\frac{na^3}{\pi}}. \quad (43)$$

The fractional depletion is approximately 2/3 of the value obtained from the Popov theory. It turns out that this is the largest change in the condensate depletion, since the effects of phase fluctuations decrease with increasing temperature. The critical temperature T_{BEC} is found by taking the limit $n_0 \rightarrow 0$ in Eqs. (8) and (9). These expressions then reduce to the same expressions for the density and chemical potential as in the Popov theory. This implies that our critical temperature for Bose-Einstein condensation coincides with that obtained in Popov theory, i.e., the ideal gas result

$$T_{\text{BEC}} = \frac{2\pi \hbar^2}{mk_B} \left[\frac{n}{\zeta\left(\frac{3}{2}\right)} \right]^{2/3}, \quad (44)$$

where $\zeta\left(\frac{3}{2}\right) \simeq 2.612$.

IV. KOSTERLITZ-THOULESS PHASE TRANSITION

In the previous section, we have compared our results using the modified many-body T-matrix theory with established results in one, two, and three dimensions in the Popov approximation. Due to the mean-field nature of the modified many-body T-matrix theory, the Kosterlitz-Thouless transition is absent and a nontrivial solution of the equation of state exists even if the superfluid density n_s obeys $n_s \Lambda^2 < 4$. In this section, we correct for this by explicitly including the effects of vortex pairs in the phase fluctuations. The idea is to use the modified many-body T-matrix theory to determine the initial values of the superfluid density and the vortex fugacity, and to carry out a renormalization-group calculation to find the fully renormalized values of these quantities. In this manner we can for example calculate the critical temperature T_c for the Kosterlitz-Thouless transition given the scattering length a and density n .

Let us for completeness first briefly sketch the derivation of the renormalization group equations for the superfluid density and the vortex fugacity [29]. Consider the velocity field of a vortex where the core is centered at the positions \mathbf{x}_i , which we for simplicity take to lie on a lattice with an area of the unit cell equal to Ω . By rotating the velocity field by ninety degrees we can map it onto the electric field of a point charge in two dimensions. Since the total energy in both systems is proportional to the square of the field integrated over space, there is complete analogy between a system of vortices and a two-dimensional Coulomb gas. This analogy is very useful and we will take advantage of it in the following. The total vorticity corresponds to the total charge of the Coulomb gas. For the analogous two-dimensional neutral Coulomb gas on a square lattice, the partition function can be written as

$$Z = \sum_{\{\mathbf{x}_i, n_i\}} e^{-\beta \left(\sum_{i \neq j} V(\mathbf{x}_i - \mathbf{x}_j) n_i n_j - E_c \sum_j n_j^2 \right)}, \quad (45)$$

where $V(\mathbf{x}_i - \mathbf{x}_j) = -2\pi \hbar^2 n_s \ln(|\mathbf{x}_i - \mathbf{x}_j|/\xi)/m$ is the Coulomb interaction between two unit point charges in two dimensions, n_s is the superfluid density, and E_c is the energy associated with the spontaneous creation of a charge, i.e., it is the core energy of the vortices. The summation is over all possible configurations of charges n_i at positions \mathbf{x}_i on the lattice. The partition function can be rewritten in a field-theoretic fashion in terms of the electrostatic potential $\phi(\mathbf{x})$ and the fugacity $y = e^{-\beta E_c}$ as

$$Z = \sum_{\{\mathbf{x}_j, n_j\}} \int \mathcal{D}\phi e^{-\int d\mathbf{x} \frac{1}{2} K' (\nabla \phi(\mathbf{x}))^2} \times e^{-i\beta \sum_j n_j \phi(\mathbf{x}_j)} y^{\sum_j n_j^2}, \quad (46)$$

where $K' = (2\pi)^2 m / \hbar^2 k_B T n_s$. In the limit where $y \ll 1$, the charge density is very low, and thus only $n_j = 0, \pm 1$ contribute to the partition function. We can then write

$$\begin{aligned} Z &\simeq \int \mathcal{D}\phi e^{-\int d\mathbf{x} \frac{1}{2} K' (\nabla\phi)^2} \prod_j \left[1 + y \exp(i\beta\phi(\mathbf{x}_j)) \right. \\ &\quad \left. + y \exp(-i\beta\phi(\mathbf{x}_j)) + \dots \right] \\ &\simeq \int \mathcal{D}\phi e^{-\int d\mathbf{x} [\frac{1}{2} K' (\nabla\phi)^2 - g \cos(\beta\phi)]}, \end{aligned} \quad (47)$$

where $g = 2y/\Omega$. It is convenient to introduce a dimensionless dielectric constant K that is related to K' by $K = \beta^2 / 4\pi^2 K' = n_s \Lambda^2 / 2\pi$ where Λ is the thermal wavelength.

The renormalization group equations for K , which is thus proportional to the superfluid density, and the fugacity y can now be obtained by performing the usual momentum-shell integrations. For the Sine-Gordon model derived in Eq. (47), this results in

$$\frac{dK^{-1}(l)}{dl} = 4\pi^3 y^2(l) + O(y^3), \quad (48)$$

$$\frac{dy(l)}{dl} = [2 - \pi K(l)] y(l) + O(y^2). \quad (49)$$

The renormalization group equations to leading order in the variables $K(l)$ and $y(l)$ were first obtained by Kosterlitz [30], while the next-to-leading order terms were derived by Amit *et al.* [31]. The flow equations are not significantly changed by including the higher-order corrections and we do not include them in the following.

The renormalization group equations (48) and (49) can be solved analytically by separation of variables and the solution is

$$y^2(l) - \frac{1}{2\pi^3} \left[\frac{2}{K(l)} + \pi \log(K(l)) \right] = C, \quad (50)$$

where the integration constant C is determined by the initial conditions. For the critical trajectory it can be calculated by evaluating the left-hand side at the fixed point $(y(\infty), K(\infty)) = (0, 2/\pi)$. In this manner, we find $C = [\log(\pi/2) - 1]/2\pi^2 \simeq -0.0278$. In Fig 2, we show the flow of the Kosterlitz renormalization group equations. There is a line of fixed points $y(\infty) = 0$ and $K(\infty) \geq 0$. The fixed point $(y(\infty), K(\infty)) = (0, 2/\pi)$ corresponds to the critical condition for the Kosterlitz-Thouless transition, where the vortices start to unbind and superfluidity disappears. Physically this can be understood from the fact that below the transition the fugacity renormalizes to zero, which implies that at the largest length scales single vortices cannot be created by thermal fluctuations. They are therefore forced to occur in pairs.

The initial conditions for the renormalization group equations are

$$K(0) = \frac{\hbar^2 n_0}{m k_B T}, \quad (51)$$

$$y(0) = e^{-\beta E_c}, \quad (52)$$

where n_0 is the quasicondensate density and E_c is the core energy of a vortex. Both are obtained from the modified many-body T-matrix theory considered previously. Writing the order parameter for a vortex configuration as $\psi_0(\mathbf{x}) = \sqrt{n_0} f(x/\xi) e^{i\vartheta}$, where ϑ is the azimuthal angle, the core energy of a vortex follows from the Gross-Pitaevskii energy functional. It reads

$$E_c = \frac{\hbar^2}{2m} n_0 \pi \int_0^\infty dx x \left[(1 - f^2)^2 + 2 \left(\frac{df}{dx} \right)^2 \right]. \quad (53)$$

The dimensionless integral was evaluated by Minnhagen and Nylén, and takes the value 1.56 [32].

Using the solution to the flow equations (50) and the initial conditions, we can calculate the temperature for the Kosterlitz-Thouless transition given the scattering length a and the density of the system. In the following, we consider again atomic hydrogen. In Fig. 3, we show the critical temperature as a function of density for $a = 2.4a_0$. We see that the critical temperature is essentially proportional to the density of the system. This can be seen in more detail in Fig. 4, where we plot $n\Lambda_c^2$ as a function of n . It is clear from this figure that $n\Lambda_c^2$ indeed changes only slightly over the density range considered.

To understand the physics of the calculation better, we show in Fig. 5 the quasicondensate fraction n_0/n following from the many-body T -matrix theory as a function of temperature for a total density $n = 1.25 \times 10^{13} \text{cm}^{-2}$. In addition, we show the superfluid density n_s as calculated from the renormalization-group procedure explained previously. The Kosterlitz-Thouless transition takes place when n_s lies on the line given by $n_s \Lambda^2 = 4$. Noticing that the left-hand side of Eq. (50) is a function of $n_0 \Lambda^2$ only and solving the equation with respect to $n_0 \Lambda^2$ using the value of C at the transition, we obtain the condition $n_0 \Lambda^2 \simeq 6.65$ for the Kosterlitz-Thouless transition. It is therefore also seen in Fig. 5 that the Kosterlitz-Thouless transition takes place when the line given by $n_0 \Lambda^2 \simeq 6.65$ intersects with the curve for n_0 .

V. TRAPPED BOSE GASES

In this section, we generalize the theory presented in Secs. II and III to inhomogeneous Bose gases. We also apply the results to a trapped one-dimensional Bose gas. We start by generalizing our previous expressions for the total density, Eq. (8), and the phase fluctuations, Eq. (10), to the inhomogeneous case. To do so we first consider the Gross-Pitaevskii equation

$$\left[-\frac{\hbar^2}{2m}\nabla^2 + V^{\text{ext}}(\mathbf{x}) + T^{\text{MB}}(-2\mu(\mathbf{x}))|\psi_0(\mathbf{x})|^2 + 2T^{\text{MB}}(-\mu(\mathbf{x}))n'(\mathbf{x}) \right] \psi_0(\mathbf{x}) = \mu\psi_0(\mathbf{x}) , \quad (54)$$

which generalizes Eq. (8) to trapped Bose condensates. Here the local chemical potential equals $\mu(\mathbf{x}) = \mu - V^{\text{ext}}(\mathbf{x})$. The noncondensed density $n'(\mathbf{x})$ is to be determined by solving the Bogoliubov-de Gennes equations

$$\hbar\omega_j u_j(\mathbf{x}) = \left[-\frac{\hbar^2}{2m}\nabla^2 + V^{\text{HF}}(\mathbf{x}) - \mu \right] u_j(\mathbf{x}) + T^{\text{MB}}(-2\mu(\mathbf{x}))n_0(\mathbf{x})v_j(\mathbf{x}) , \quad (55)$$

$$-\hbar\omega_j v_j(\mathbf{x}) = \left[-\frac{\hbar^2}{2m}\nabla^2 + V^{\text{HF}}(\mathbf{x}) - \mu \right] v_j(\mathbf{x}) + T^{\text{MB}}(-2\mu(\mathbf{x}))n_0(\mathbf{x})u_j(\mathbf{x}) , \quad (56)$$

where $n_0(\mathbf{x}) = |\psi_0(\mathbf{x})|^2$ and the Hartree-Fock potential $V^{\text{HF}}(\mathbf{x})$ is given by

$$V^{\text{HF}}(\mathbf{x}) = V^{\text{ext}}(\mathbf{x}) + 2T^{\text{MB}}(-\mu(\mathbf{x}))n'(\mathbf{x}) + 2T^{\text{MB}}(-2\mu(\mathbf{x}))n_0(\mathbf{x}) . \quad (57)$$

The functions u_j and v_j are the usual Bogoliubov particle and hole amplitudes respectively, which are chosen to be real here. In some cases, for instance when ψ_0 describes a vortex, we cannot choose these amplitudes real and our equations are easily generalized to incorporate that fact.

In terms of the Bogoliubov amplitudes, the expression for the total density in Eq. (8) reads

$$n(\mathbf{x}) = n_0(\mathbf{x}) + \sum_j \left[(u_j(\mathbf{x}) + v_j(\mathbf{x}))^2 N(\hbar\omega_j) + v_j(\mathbf{x})(v_j(\mathbf{x}) + u_j(\mathbf{x})) + \frac{T^{\text{MB}}(-2\mu(\mathbf{x}))n_0(\mathbf{x})}{2\epsilon_j + 2\mu(\mathbf{x})}(\phi_j(\mathbf{x}))^2 \right] . \quad (58)$$

Here, ϕ_j is the large- j or high-energy limit of u_j which can be obtained by neglecting the interaction terms in Eq. (55), namely

$$\epsilon_j \phi_j(\mathbf{x}) = \left(-\frac{\hbar^2}{2m}\nabla^2 + V^{\text{ext}}(\mathbf{x}) - \mu \right) \phi_j(\mathbf{x}) . \quad (59)$$

In the large- j limit, we also have

$$v_j(\mathbf{x}) = -\frac{T^{\text{MB}}(-2\mu(\mathbf{x}))n_0(\mathbf{x})}{2\epsilon_j} \phi_j(\mathbf{x}) . \quad (60)$$

It is clear that the expression of Eq. (58) for the total density is ultraviolet finite since the second and third term cancel each other in the large- j limit.

Finally, the phase fluctuations in the trapped case are determined by $\langle \hat{\chi}(\mathbf{x})\hat{\chi}(\mathbf{x}') \rangle$ which is given by

$$\begin{aligned} \langle \hat{\chi}(\mathbf{x})\hat{\chi}(\mathbf{x}') \rangle = & -\sum_j \frac{1}{2\sqrt{n_0(\mathbf{x})n_0(\mathbf{x}')}} \left\{ u_j(\mathbf{x}')v_j(\mathbf{x}) [1 + 2N(\hbar\omega_j)] \right. \\ & + \left[\frac{T^{\text{MB}}(-2\mu(\mathbf{x}))n_0(\mathbf{x})}{2\epsilon_j + 2\mu(\mathbf{x})} \right] \phi_j(\mathbf{x}')\phi_j(\mathbf{x}) \\ & + u_j(\mathbf{x})v_j(\mathbf{x}') [1 + 2N(\hbar\omega_j)] \\ & \left. + \left[\frac{T^{\text{MB}}(-2\mu(\mathbf{x}'))n_0(\mathbf{x}')}{2\epsilon_j + 2\mu(\mathbf{x}')} \right] \phi_j(\mathbf{x})\phi_j(\mathbf{x}') \right\} . \end{aligned} \quad (61)$$

In particular the normalized form of the off-diagonal one-particle density matrix of Eq. (20) becomes for large distances $|\mathbf{x} - \mathbf{x}'|$ equal to

$$g^{(1)}(\mathbf{x}, \mathbf{x}') = \exp(-\langle [\hat{\chi}(\mathbf{x}) - \hat{\chi}(\mathbf{x}')]^2 \rangle / 2) . \quad (62)$$

A. Density profiles

We are now ready to calculate the total density profile by solving Eqs. (54) and (58) selfconsistently. In the remainder of the paper, we restrict ourselves to one-dimensional harmonic traps with, therefore,

$$V^{\text{ext}}(z) = \frac{1}{2}m\omega_z^2 z^2 . \quad (63)$$

For simplicity we use the local-density approximation, which allows us to calculate the densities directly using the many-body generalization of Eq. (8), and Eq. (12). In Fig. 6 the total density profile is shown at four different values of the temperature. For the four different temperatures each of the four curves is composed of two parts. The first part near the center of the trap represents the superfluid part of the gas and contains the (quasi)condensate. The other part consists only of the noncondensed atoms. The small discontinuity between the two parts is caused by the use of two different equations of state for the superfluid and thermal phases of the gas. In the following we call the position of the discontinuity the temperature-dependent Thomas-Fermi radius of the (quasi)condensate. For distances below the discontinuity we use the above-mentioned equations, while for distances above the discontinuity, we simply use

$$n(z) = \int_{-\infty}^{\infty} \frac{dk}{2\pi} N(\epsilon_k + m\omega_z^2 z^2 / 2 + 2nT^{\text{MB}}(-\hbar\Sigma(z)) - \mu) . \quad (64)$$

For all these curves $\mu = 30\hbar\omega_z$. The remaining parameters used here are those of the experiment of Görlitz *et al.* [1]. In particular, we have used ^{23}Na in the trap with $\omega_z = 2\pi \times 3.5$ rad/sec, $l_z = \sqrt{\hbar/m\omega_z} \simeq 1.12 \times 10^{-5}\text{m}$. The three-dimensional s -wave scattering length is $a \simeq$

2.75 nm which is related to the one-dimensional scattering length κ^{-1} defined by $T^{2B}(-2\mu) = 4\pi\kappa\hbar^2/m$. For harmonic confinement, we have $\kappa = a/2\pi l_\perp^2$, where l_\perp is the harmonic oscillator length of the axially symmetric trap in the direction perpendicular to the z -axis. We have used $\omega_\perp = 2\pi \times 360$ rad/sec and $l_\perp = \sqrt{\hbar/m\omega_\perp} \simeq 1.10 \times 10^{-6}$ m.

As expected, the temperature-dependent Thomas-Fermi radius decreases with increasing the temperature. At the temperature when this radius vanishes the one-dimensional system reaches the crossover temperature for the formation of a (quasi)condensate. We have calculated this crossover temperature for different values of the scattering length at a constant value of the number of atoms, the latter being fixed by adjusting the chemical potential. In Fig. 7, we show the result of this calculation, and plot the crossover temperature T_{QC} and the chemical potential against the scattering length. The inset in Fig. 7 shows that on a double logarithmic scale the temperature T_{QC} is clearly not a straight line indicating that the relation between T_{QC} and κ is not a simple power law and may contain logarithmic dependence. It is shown in Ref. [33] that for $a = 0$, the transition temperature T_{QC} should satisfy $T_{QC} = N\hbar\omega_z/k_B \ln(2N)$, where N is the number of atoms. In the case of Fig. 7 we have $N = 950$, which leads to $T_{QC} \simeq 164T_0$ for an ideal gas. Of course, this limit is not obtained in Fig. 7 because our calculation is based on a local-density approximation, which will always break down for sufficiently small values of κ . On the other hand, the curve for the chemical potential becomes almost a straight line on a double logarithmic scale. A calculation of the slope of this line shows that the slope starts at a value slightly larger than $2/3$ at the lower end of the curve and saturates at this value near the upper end. The value $2/3$ is what we expect, since in the Thomas-Fermi limit it is easy to show that $\mu = (3\pi/\sqrt{2})^{2/3}(N\kappa)^{2/3}\hbar\omega_z \simeq 3.5(N\kappa)^{2/3}\hbar\omega_z$. Calculating similar curves for different values of N we actually find numerically that $\mu \simeq 3.2(N\kappa)^{2/3}\hbar\omega_z$.

B. Phase fluctuations

The aim of this section is to calculate the normalized off-diagonal density matrix given by Eq. (62). This function expresses the coherence in the system. It is calculated by solving the Bogoliubov-de Gennes equations in Eqs. (55) and (56) using the density profile calculated in the previous subsection. Specifically from the (quasi)condensate density profile n_0 , we determine a temperature-dependent Thomas-Fermi radius. This radius is then used to calculate the phase fluctuations at that specified temperature in the following manner.

We start by employing the following scaling: lengths are scaled to the trap length $l_z = (\hbar/m\omega_z)^{1/2}$, frequencies to ω_z , energies to $\hbar\omega_z$, and densities to $4\pi/l_z$. With

this scaling, the Bogoliubov-de Gennes equations take the dimensionless form

$$\omega_j u_j = \left(-\frac{1}{2} \frac{d^2}{dz^2} + \frac{1}{2} z^2 - \mu + 2\kappa n \right) u_j - \kappa n_0 v_j, \quad (65)$$

$$-\omega_j v_j = \left(-\frac{1}{2} \frac{d^2}{dz^2} + \frac{1}{2} z^2 - \mu + 2\kappa n \right) v_j - \kappa n_0 u_j. \quad (66)$$

Using the same scaling, the Gross-Pitaevskii equation takes the form

$$\left[-\frac{1}{2} \frac{d^2}{dz^2} + \frac{1}{2} z^2 - \mu + \kappa(n_0 + 2n') \right] \sqrt{n_0} = 0. \quad (67)$$

Next we define $F_j(z) = u_j(z) + v_j(z)$ and $G_j(z) = u_j(z) - v_j(z)$, and derive from Eqs. (65) and (66) two equations for $F_j(z)$ and $G_j(z)$, namely

$$\frac{d^4 F}{dz^4} - 2(f+g) \frac{d^2 F}{dz^2} - 4 \frac{dg}{dz} \frac{dF}{dz} - \left(4\omega_j^2 + 2 \frac{d^2 g}{dz^2} - 4gf \right) F = 0, \quad (68)$$

$$\frac{d^4 G}{dz^4} - 2(f+g) \frac{d^2 G}{dz^2} - 4 \frac{df}{dz} \frac{dG}{dz} - \left(4\omega_j^2 + 2 \frac{d^2 f}{dz^2} - 4gf \right) G = 0, \quad (69)$$

where the functions $f(z)$ and $g(z)$ are given by

$$f = \frac{1}{2} z^2 + 2\kappa n - \mu + \kappa n_0, \quad (70)$$

$$g = \frac{1}{2} z^2 + 2\kappa n - \mu - \kappa n_0. \quad (71)$$

For our purposes we can use the Thomas-Fermi approximation which neglects the derivative term in Eq. (67). Hence

$$\left[\frac{1}{2} z^2 - \mu + \kappa(n_0 + 2n') \right] \sqrt{n_0} = 0. \quad (72)$$

In this limit, the functions $f(z)$ and $g(z)$ are given by $f(z) = 2\kappa n_0(z)$ and $g(z) = 0$. In the Thomas-Fermi approximation, we substitute these values for $f(z)$ and $g(z)$ into Eqs. (68) and (69) and neglect the fourth-order derivative terms. These Equations thus take the form

$$\kappa n_0 \frac{dF_j^2}{dz^2} + \omega_j^2 F_j = 0, \quad (73)$$

$$\frac{d^2(\kappa n_0 G_j)}{dz^2} + \omega_j^2 G_j = 0. \quad (74)$$

In Ref. [34], it was shown that $\sqrt{\kappa n_0(z)} G_j(z)$ corresponds to density fluctuations and $F_j(z)/\sqrt{\kappa n_0(z)}$ corresponds to phase fluctuations in the hydrodynamic approach [35]. We therefore define the function $h_j(z)$

$$h_j = \sqrt{\kappa n_0} G_j = F_j / \sqrt{\kappa n_0} . \quad (75)$$

Substituting this back in Eqs. (73) and (74) both equations reduce to a single equation for $h_j(z)$, namely

$$\kappa n_0 \frac{d^2 h_j}{dz^2} + \kappa \frac{dn_0}{dz} \frac{dh_j}{dz} + \omega_j^2 h_j = 0 . \quad (76)$$

This equation can finally be simplified using the Thomas-Fermi expression for $\kappa n_0(z)$ from Eq. (72), namely $\kappa n_0(z) \simeq \mu' - z^2/2$ where $\mu' = \mu - 2\kappa n'(0)$. Note that we have made the approximation that we take $n'(z)$ to be equal to its value at the center, namely $n'(0)$. This approximation is justified in view of the fact that the presence of the condensate repels the atoms from the noncondensate atoms from the center of the trap. This is also supported by a numerical solution of Eqs. (8) and (12), where we find that $n'(z) \ll n_0(z)$, except at the Thomas-Fermi radius where they become of the same order. Moreover, the slope of $n'(z)$ is small for distances close to the center. Thus, the last equation becomes

$$(1 - y^2) \frac{d^2}{dy^2} h_j(y) - 2y \frac{d}{dy} h_j(y) + 2\omega_j^2 h_j(y) = 0 , \quad (77)$$

where $y = z/R_{\text{TF}}(T)$ and $R_{\text{TF}}(T) = \sqrt{2\mu'(T)}$ is the Thomas-Fermi radius

In the following, we reinstate the units. Interestingly, Eq. (77) is the Legendre equation with the Legendre polynomials as solutions:

$$h_j(z) = P_j(z/R_{\text{TF}}) = P_j(y) , \quad (78)$$

where the energy eigenvalues are

$$\hbar\omega_j = \sqrt{\frac{j(j+1)}{2}} \hbar\omega_z , \quad j = 0, 1, 2, \dots . \quad (79)$$

The normalization condition for the Bogoliubov amplitudes is

$$\int_{-R_{\text{TF}}}^{R_{\text{TF}}} dz [|u_j|^2(z) - |v_j|^2(z)] = 1 , \quad (80)$$

which leads to

$$F_j(z) = \frac{1}{\sqrt{R_{\text{TF}}}} \sqrt{\frac{(j+1/2)\mu'}{\hbar\omega_j}} \sqrt{1-y^2} P_j(y) , \quad (81)$$

$$G_j(z) = \frac{1}{\sqrt{R_{\text{TF}}}} \sqrt{\frac{(j+1/2)\hbar\omega_j}{\mu'}} \frac{P_j(y)}{\sqrt{1-y^2}} . \quad (82)$$

These expressions are in agreement with those obtained in Ref. [36]. Consequently, we find

$$u_j(z) = \frac{1}{2} \left(A_j \sqrt{1-y^2} + \frac{B_j}{\sqrt{1-y^2}} \right) P_j(y) , \quad (83)$$

$$v_j(z) = \frac{1}{2} \left(A_j \sqrt{1-y^2} - \frac{B_j}{\sqrt{1-y^2}} \right) P_j(y) , \quad (84)$$

where

$$A_j = \frac{1}{\sqrt{R_{\text{TF}}}} \sqrt{\frac{(j+1/2)\mu'}{\hbar\omega_j}} \quad (85)$$

$$B_j = \frac{1}{\sqrt{R_{\text{TF}}}} \sqrt{\frac{(j+1/2)\hbar\omega_j}{\mu'}} . \quad (86)$$

The expression for the phase fluctuations in Eq. (61) now reads, after neglect of the quantum contribution,

$$\begin{aligned} \langle [\hat{\chi}(z) - \hat{\chi}(z')]^2 \rangle = & \frac{4\pi\kappa l_z^4}{R_{\text{TF}}^2} \sum_{j=0} N(\hbar\omega_j) \left\{ A_j^2 [P_j(y) - P_j(y')]^2 \right. \\ & \left. - B_j^2 \left[\frac{P_j(y)}{1-y^2} - \frac{P_j(y')}{1-y'^2} \right]^2 \right\} . \end{aligned} \quad (87)$$

It should be noted that the first term in this sum, $j = 0$, does not diverge as one might think at first instance. It actually vanishes and the sum can start from $j = 1$. Physically, this is a result of the fact that the global phase does not influence the phase fluctuations.

For the four values of temperature used in Fig. 6, we insert the corresponding $R_{\text{TF}}(T)$ in Eq. (87) to calculate the phase correlation function $g^{(1)}(0, z)$. In Fig. 8, we plot this quantity and we see that at sufficiently low temperatures the phase correlation function decreases only slightly over the condensate size. This indicates that a true condensate can exist at sufficiently low temperatures for interacting trapped one-dimensional Bose gases.

C. Comparison with exact results

We next compare the above results to predictions based on a Langevin field equation for the order parameter of a trapped, one-dimensional condensate in contact with a three-dimensional Bose gas that acts as a “heat bath”. Such a situation can be created experimentally in a magnetically trapped three-dimensional system, by using a laser beam to provide an additional optical potential along two of the directions. The laser beam then needs to be focused such that the motion of the system freezes out along these directions. The gas in the potential “dimple” provided by the laser then indeed becomes an effectively one-dimensional condensate, in contact with the three-dimensional thermal cloud in the magnetic trap, which acts as its heat bath. The dynamics of the order parameter is governed in this case by [14,37]

$$i\hbar \frac{\partial \Phi(z, t)}{\partial t} = \left[-\frac{\hbar^2 \nabla^2}{2m} + V^{\text{ext}}(z) - \mu - iR(z, t) + g|\Phi(z, t)|^2 \right] \Phi(z, t) + \eta(z, t), \quad (88)$$

where the external trapping potential in the weakly-confined direction $V^{\text{ext}}(z)$ is again given in Eq. (63) and μ is the effective chemical potential of the one-dimensional system. The one-dimensional coupling constant g is related to κ by $g = 4\pi\kappa\hbar^2/m$. Physically, the function $iR(z, t)$ describes the pumping of the one-dimensional condensate from the surrounding thermal cloud, and $\eta(z, t)$ corresponds to the associated noise with Gaussian correlations. Both these quantities depend on the one-dimensional Keldysh self-energy $\hbar\Sigma^K(z)$, as discussed in detail in Ref. [37]. For our purposes, we only need that

$$iR(z, t) = -\frac{\beta}{4}\hbar\Sigma^K(z) \times \left(-\frac{\hbar^2 \nabla^2}{2m} + V^{\text{ext}}(z) - \mu + T^{2B}|\Phi(z, t)|^2 \right), \quad (89)$$

$$\langle \eta^*(z, t)\eta(z', t') \rangle = \frac{i\hbar^2}{2}\Sigma^K(z)\delta(z - z')\delta(t - t'), \quad (90)$$

where $\langle \dots \rangle$ denotes averaging over the realizations of the noise $\eta(z, t)$. The numerical techniques employed are discussed in Ref. [37], where it also was shown that with the last two expressions, the trapped gas relaxes to the correct equilibrium, as ensured by the fluctuation-dissipation theorem. To simplify the numerics, the non-condensed part in the dimple is here allowed to relax to the “classical” value $N(\epsilon) = [\beta(\epsilon - \mu)]^{-1}$, and the comparison to the previous mean-field predictions is therefore carried out by making the same approximation in the calculation of both $n_0(z)$ and $n'(z)$. The normalized first-order correlation function at equal time $g^{(1)}(0, z)$ corresponding to the previously computed phase correlation function, is calculated via numerical autocorrelation measurements, i.e.,

$$g^{(1)}(0, z, t) = \frac{\langle \Phi^*(0, t)\Phi(z, t) \rangle}{\sqrt{\langle |\Phi(0, t)|^2 \rangle \langle |\Phi(z, t)|^2 \rangle}}, \quad (91)$$

where the brackets again denote averaging over the different realizations of the noise. Of course, the time t must be sufficiently large so that the gas has relaxed to thermal equilibrium and $g^{(1)}(0, z, t)$ is independent of time.

In Figs. 9 and 10, we show the comparison of the many-body T -matrix theory to the above Langevin calculations, for the same temperatures used in Figs. 6 and 8. In Fig. 9 we compare the Langevin densities $\langle |\Phi(z, t)|^2 \rangle$ to our classical mean-field density $n(z)$. This yields excellent agreement at low temperatures, except for a small region around the discontinuity in the mean-field theory, which can be understood from the fact that the local-density approximation always fails in a small region near

the edge of the Thomas-Fermi radius. As expected, this region increases with increasing temperature. For $T = 50$ nK, Fig. 9 further shows the deviation of the “classical” prediction of our mean-field theory from the “quantum” one calculated previously in Sec. V A and displayed in Fig. 6. Finally, Fig. 10 shows the corresponding phase correlation functions as a function of position. Here we also find very good agreement in the entire temperature range. Note that the phase correlation functions are essentially indistinguishable for both classical and quantum treatments of the thermal cloud.

It is interesting to note that the Langevin method yields continuous curves at the expense of computational time, due to the large number of independent runs that are required to reduce the statistical error. However, the Langevin method enables also a direct calculation of the time-dependent correlation properties via temporal autocorrelation measurements. Results of such studies, which are of the interest for the physics of an atom laser, will be presented in a separate publication [38].

Finally, it is worth mentioning again that in obtaining our analytical expressions for the phase fluctuations and the density in sections II and V, we have used the many-body T -matrix for the interatomic interactions. As mentioned in section II B the many-body effects are important in one and two dimensions. To appreciate this importance, we recalculate the density profiles and phase fluctuations using the two-body T -matrix. Thus for distances below R_{TF} the differences are due to Eq. (11), whereas for distances above R_{TF} they are a result of Eq. (29). In Figs. 11 and 12 it is clearly seen that the inclusion of many-body effects has led to a better agreement with the exact Langevin results. Moreover, the many-body corrections become more pronounced at higher temperatures. In Fig. 13, we show how the renormalized interatomic interaction strength $T^{\text{MB}}(-2\mu(z))$ depends on position. We notice that the effects of this renormalization becomes most significant near the edge of the condensate and for temperatures closer to the transition temperature, as expected from the results of Refs. [19,39].

VI. CONCLUSIONS

The Popov theory suffers from infrared divergences in the equation of state at all temperatures in one dimension and at any nonzero temperature in two dimensions. These infrared divergences can be traced to an inaccurate treatment of the phase fluctuations. We have proposed a new mean-field theory for dilute Bose gases, in which the phase fluctuations are treated exactly. We have also used this to arrive at an improved many-body T -matrix theory. The resulting equation of state is free of infrared divergences and the theory can thus be applied in any

dimension. Our modified many-body T -matrix theory is capable of reproducing exact results in one dimension and the results in three dimensions are to a large extent the same as those predicted by Popov theory. We have used the theory to calculate the reduction of the recombination rate of a spin-polarized two-dimensional hydrogen system. Comparing our calculated rate with the observed values we found reasonable agreement, although more work is required to make a detailed comparison.

We have also applied the theory to the Kosterlitz-Thouless phase transition. The modified many-body T -matrix theory is used to calculate initial conditions for the superfluid density and the fugacity of the vortices in a renormalization group calculation that incorporates the physics of vortex pairs. We have calculated the critical temperature for a fixed value of the s -wave scattering length as a function of density, and it was found that T_c increases almost linearly with density. More precisely we have obtained $n\Lambda_c^2 \simeq 7$. We believe that this result gives a lower bound on the critical temperature, since the Kosterlitz-Thouless renormalization group equations do not include quantum effects, which in principle affect nonuniversal quantities.

The modified many-body T -matrix theory was also applied to calculate density profiles and phase correlation functions of a one-dimensional trapped Bose gas for a variety of temperatures. At very low temperatures, the phase correlation function was found to decrease only very slightly over the size of the system, indicating that the equilibrium state contains a true condensate. At larger temperatures, it decreases faster, and the gas now contains only a quasicondensate. In future work, we will look in detail at this and also at the full crossover problem between one, two, and three dimensions. Finally, the densities and phase correlation functions predicted by our mean-field theory for various temperatures were compared to the corresponding predictions of a nonlinear Langevin field equation, which gives numerically exact results. The agreement was found to be very good for the entire temperature range studied.

ACKNOWLEDGMENTS

We thank Tom Bergeman, Steve Girvin, and Subir Sachdev for valuable discussions and inspiration. We also thank Simo Jaakkola and Sasha Safanov for providing us with the data of their experiment. This work was supported by the Stichting voor Fundamenteel Onderzoek der Materie (FOM), which is supported by the Nederlandse Organisatie voor Wetenschappelijk Onderzoek (NWO).

- [1] A. Görlitz, J.M. Vogels, A.E. Leanhardt, C. Raman, T. L. Gustavson, J. R. Abo-Shaeer, A. P. Chikkatur, S. Gupta, S. Inouye, T. P. Rosenband, D. E. Pritchard, and W. Ketterle, Phys. Rev. Lett. **87**, 130402 (2001).
- [2] F. Schreck, L. Khaykovich, K. L. Corwin, G. Ferrari, T. Bourdel, J. Cobizolles, and C. Salomon, Phys. Rev. Lett. **87**, 080403 (2001).
- [3] H. Ott, J. Fortagh, G. Schlotterbeck, A. Grossmann, and C. Zimmermann, Phys. Rev. Lett. **87**, 230401 (2001).
- [4] W. Hänsel, P. Hommelhoff, T. W. Hänsch, and J. Reichel, Nature **413**, 501 (2001).
- [5] W. J. Mullin, J. Low. Temp. Phys. **106**, 615 (1997).
- [6] T.-L. Ho and M. Ma, J. Low Temp. Phys. **115**, 61 (1999).
- [7] D. S. Petrov, M. Holzmann, and G.V. Shlyapnikov, Phys. Rev. Lett. **84**, 2551 (2000).
- [8] D. S. Petrov, G.V. Shlyapnikov, and J.T.M. Walraven, Phys. Rev. Lett. **85**, 3745 (2000).
- [9] N. D. Mermin and H. Wagner, Phys. Rev. Lett. **22**, 1133 (1966).
- [10] P. C. Hohenberg, Phys. Rev. **158**, 383 (1967).
- [11] V. N. Popov, Theor. Math. Phys. **11**, 565 (1972); *Functional Integrals in Quantum Field Theory and Statistical Physics*, (Reidel, Dordrecht, 1983), Chap. 6.
- [12] J. O. Andersen, U. Al Khawaja, and H. T. C. Stoof, Phys. Rev. Lett. **88**, 070407 (2002).
- [13] J. M. Kosterlitz and D. J. Thouless, J. Phys. C **6**, 1181 (1973).
- [14] H. T. C. Stoof, J. Low Temp. Phys. **114**, 11 (1999).
- [15] A. I. Safonov, S.A. Vasilyev, I. S. Yasnikov, I.I. Lukashevich, and S. Jaakkola, Phys. Rev. Lett. **81**, 4545 (1998).
- [16] H. T. C. Stoof and M. Bijlsma, Phys. Rev. E **47**, 939 (1993).
- [17] M. Schick, Phys. Rev. A **3**, 1067 (1971).
- [18] D. S. Fisher and P.C. Hohenberg, Phys. Rev. B **37**, 4936 (1988).
- [19] M. Bijlsma and H. T. C. Stoof, Phys. Rev. A **54**, 5085 (1996).
- [20] N. P. Proukakis, S. A. Morgan, S. Choi, and K. Burnett, Phys. Rev. A **58**, 2435 (1998).
- [21] H. T. C. Stoof, M. Bijlsma, and M. Houbiers, J. Res. Natl. Stand. Technol. **101**, 443 (1996).
- [22] F. D. M. Haldane, Phys. Rev. Lett. **47**, 1840 (1981).
- [23] M. Olshanii, Phys. Rev. Lett. **81**, 938 (1998).
- [24] M.D. Girardeau and E. M. Wright, Phys. Rev. Lett. **84**, 5239 (2000).
- [25] H.T.C. Stoof and M. Bijlsma, Phys. Rev. B **49**, 422 (1994).
- [26] H. T. C. Stoof, L. P. H. de Goey, W. M. H. M. Rovers, P. S. M. Kop Jansen, and B.J. Verhaar, Phys. Rev. A **38**, 1248 (1988).
- [27] Yu. Kagan, B. V. Svistunov, G. V. Shlyapnikov, JETP Lett. **42**, 209 (1985).
- [28] T. D. Lee and C. N. Yang, Phys. Rev. **105**, 1119 (1957).
- [29] S. M. Girvin, private communication.
- [30] J.M. Kosterlitz, J. Phys. C **7**, 1046 (1974).
- [31] D. J. Amit, Y.Y. Goldschmidt, and G. Grinstein, J. Phys. A, **13**, 585 (1980).
- [32] P. Minnhagen and M. Nylén, Phys. Rev. B **31**, 5768 (1985).

- [33] W Ketterle and N. J. van Druten, Phys. Rev. A **54**, 656 (1996).
- [34] A. L. Fetter and D. Rokhsar, Phys. Rev. A **57**, 1191 (1998).
- [35] S. Stringari, Phys. Rev. Lett. **77**, 2360 (1996).
- [36] D. S. Petrov, G. V. Shlyapnikov, and J. T. M. Walraven, Phys. Rev. Lett. **85**, 3745 (2000).
- [37] H. T. C. Stoof and M.J. Bijlsma, J. Low Temp. Phys. **124**, 431 (2001).
- [38] N.P. Proukakis and H.T.C Stoof, unpublished.
- [39] M. Bijlsma and H. T. C. Stoof, Phys. Rev. A **55**, 498 (1997).

FIGURES

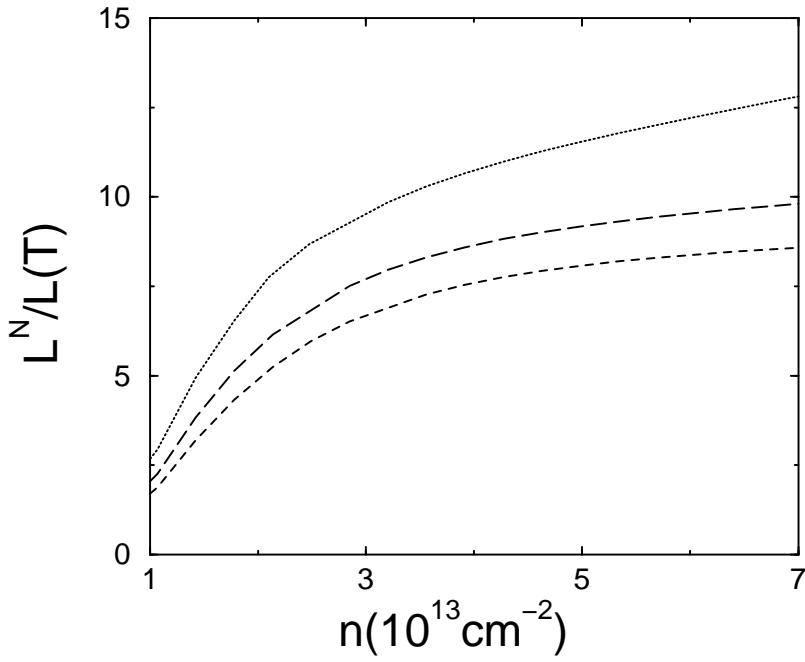


FIG. 1. Reduction of the three-body recombination rate as a function of the density for a temperature of $T = 190$ mK and three different values of the scattering length. The dotted line corresponds to $a = 2.4a_0$, the long-dashed line to $a = 1.2a_0$, and the dashed line to $a = 0.6a_0$, respectively.

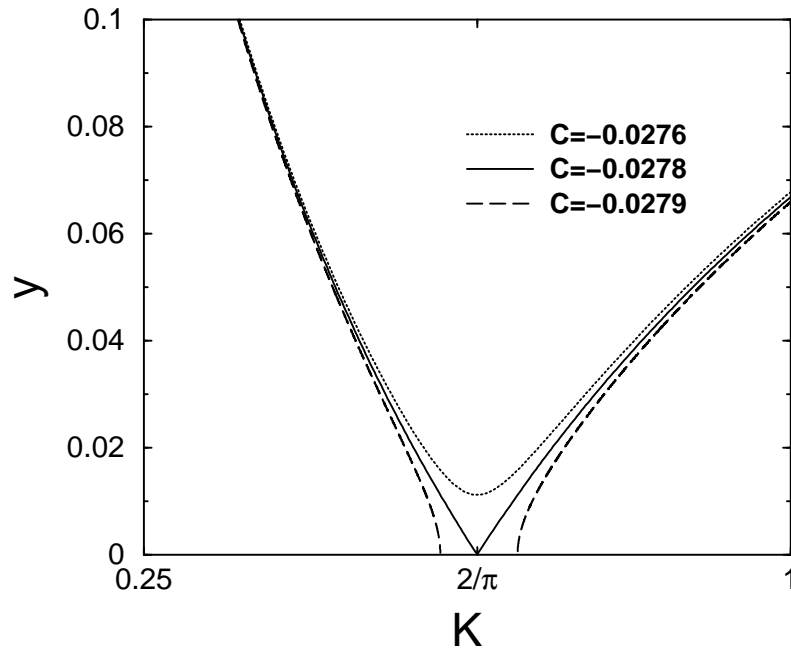


FIG. 2. Renormalization group flow for the coupling constants y and K . These curves are given by Eq. (50) for different values of C .

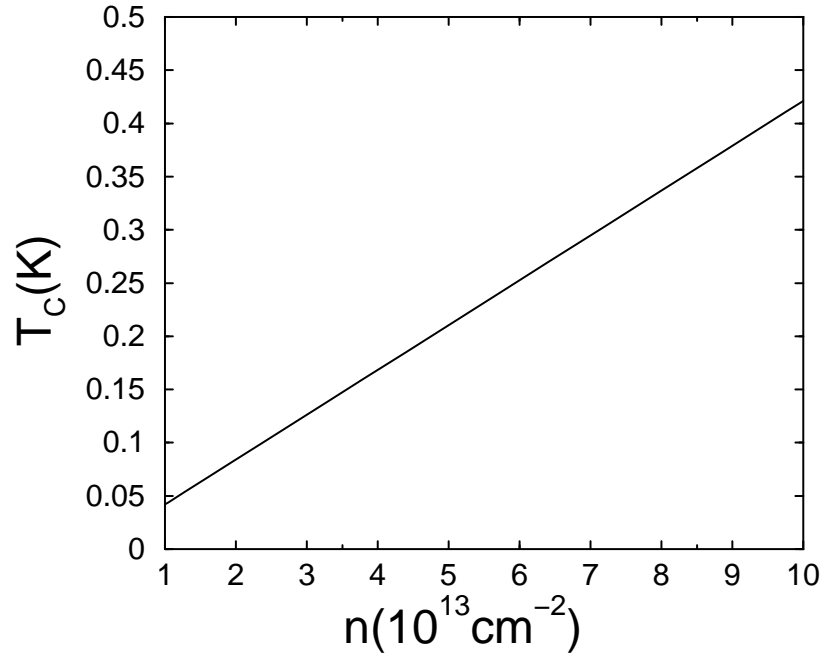


FIG. 3. The critical temperature for the Kosterlitz-Thouless transition as a function of the density for spin-polarized atomic hydrogen with $a = 2.4a_0$.

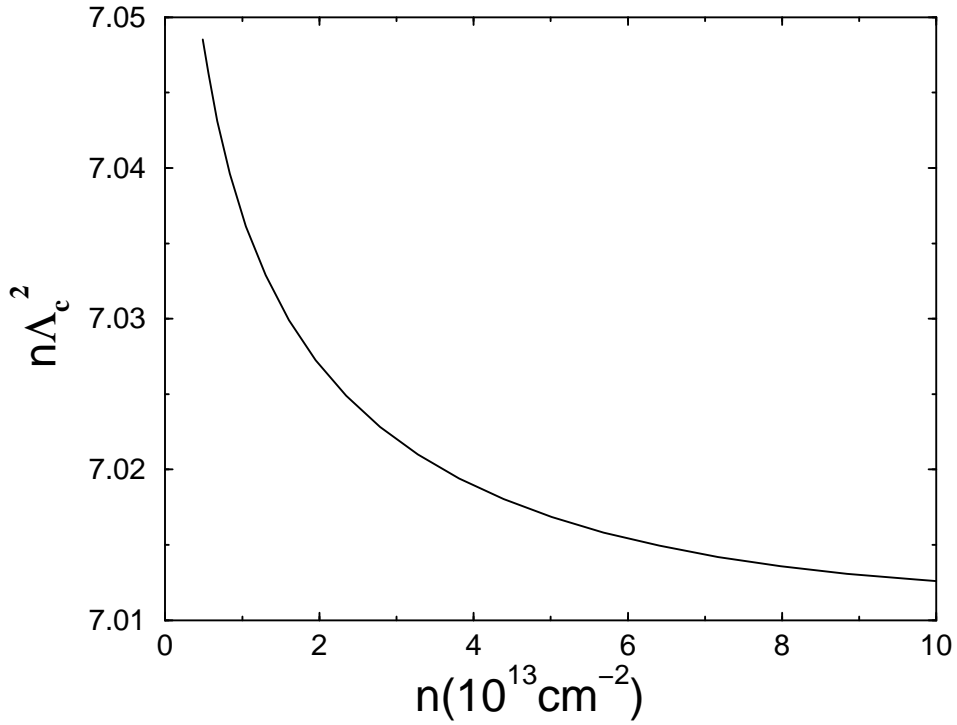


FIG. 4. The critical degeneracy parameter $n\Lambda_c^2$ as a function of the density for spin-polarized atomic hydrogen with $a = 2.4a_0$.

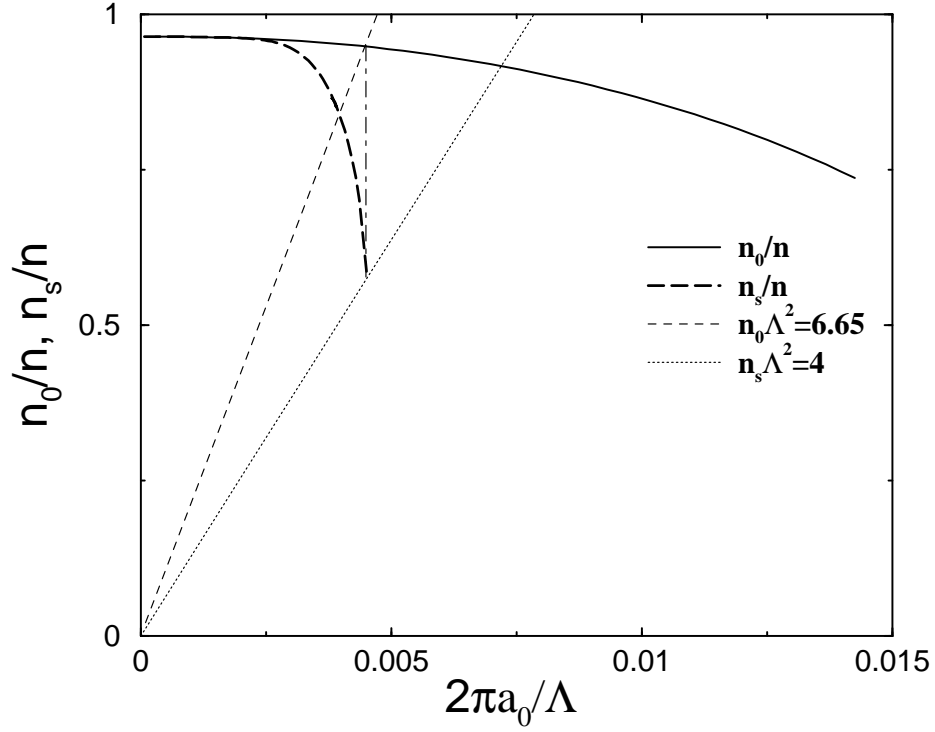


FIG. 5. Quasicondensate density n_0 (solid curve) and superfluid density n_s (long dashed curve) as a function of temperature. Also plotted are the Kosterlitz-Thouless condition $n_s\Lambda^2 = 4$ (dotted line) and the condition $n_0\Lambda^2 = 6.65$ (dashed line). The Kosterlitz-Thouless transition takes place when the dashed line intersects the solid curve. At the intersection point the long-dashed curve reaches the dotted line.

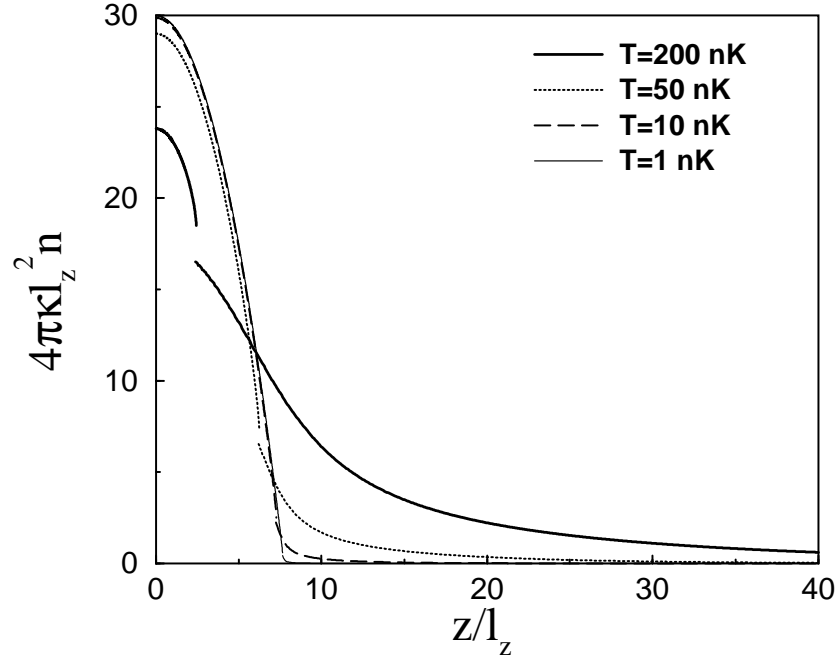


FIG. 6. Density profile of a trapped one-dimensional Bose gas at four different temperatures. The quantities l_z and κ are defined in the text.

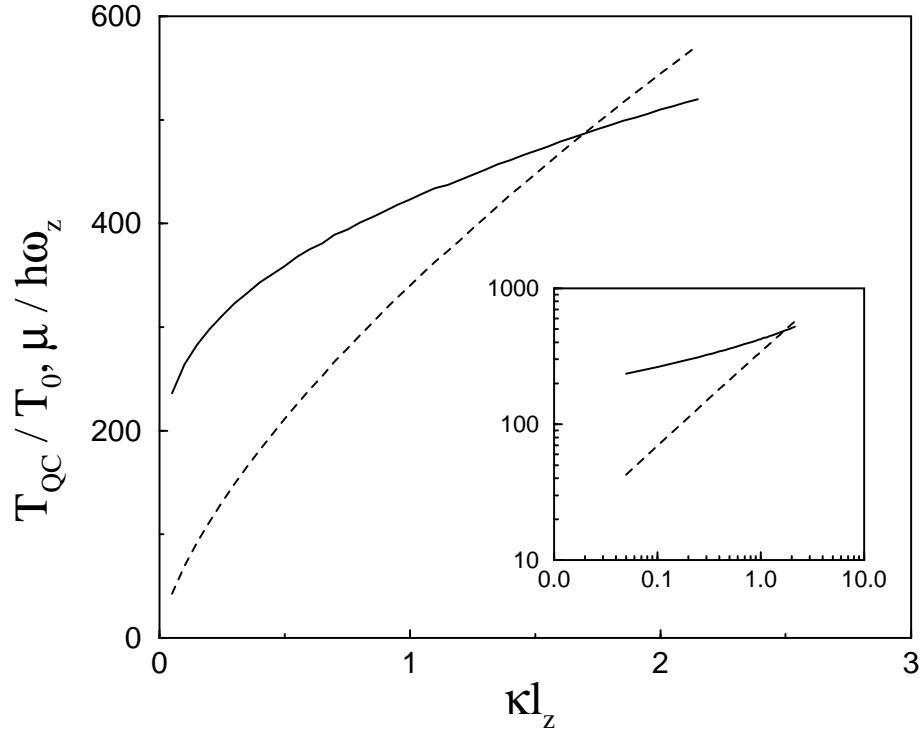


FIG. 7. The crossover temperature T_{QC} is shown with the solid curve, and the chemical potential at this temperature is shown with the dashed curve, both as a function of the coupling constant. The temperature is scaled to $T_0 = \hbar^2 / mk_B l_z^2$. The inset shows the same curves on a double logarithmic scale.

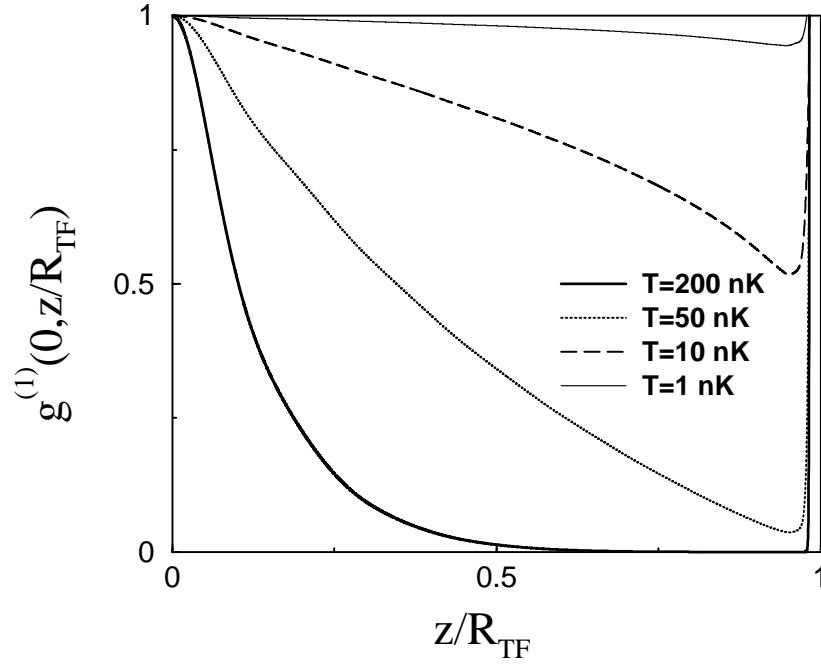


FIG. 8. Normalized first-order (phase) correlation function as a function of position for different temperatures.

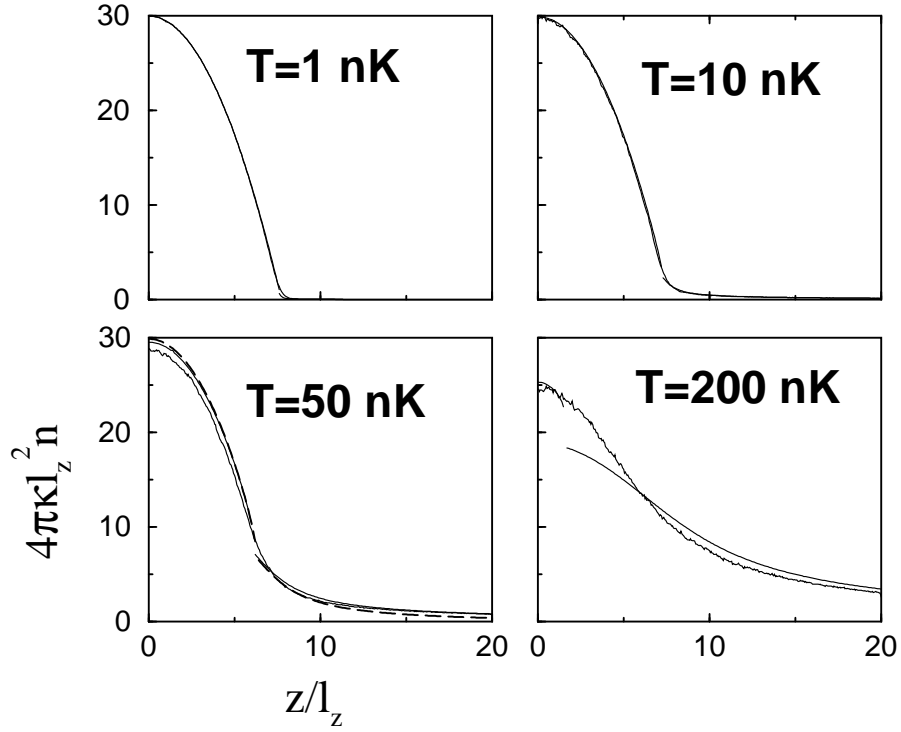


FIG. 9. Comparison of the mean-field densities profiles (solid curves) to numerical solutions of the Langevin equation in Eq. (88) (noisy curves). All the above curves are calculated using the classical approximation of the Bose-Einstein distribution function. For the $T = 50$ nK case we have also plotted the corresponding density calculated using the full Bose-Einstein distribution function (dashed curve) in order to show the difference between the classical and quantum mean-field approximations.

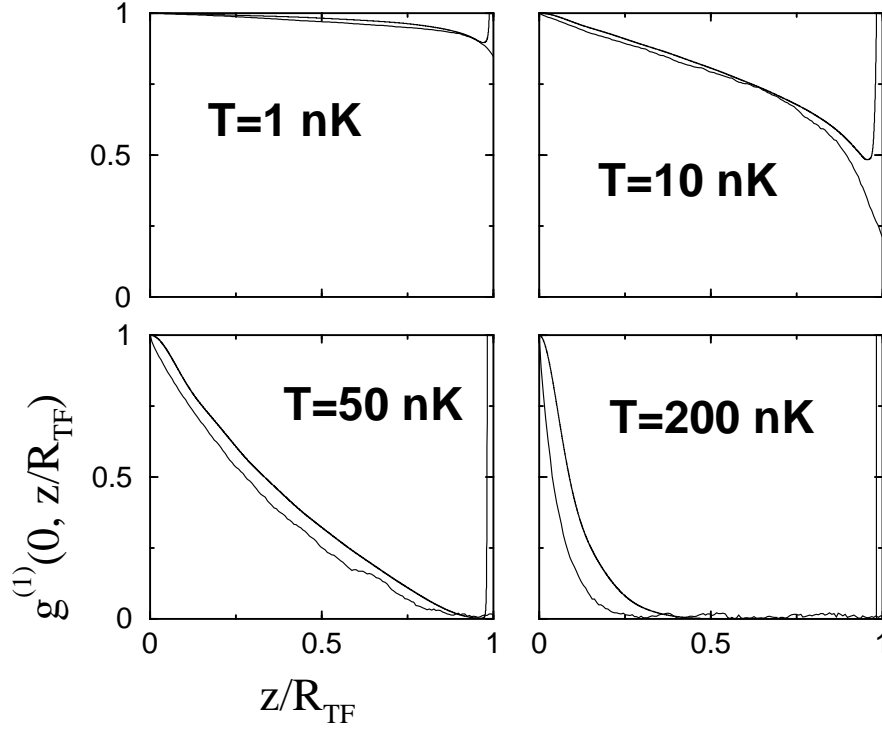


FIG. 10. Comparison of the normalized first-order (phase) correlation functions calculated using the present mean-field approach, given by the solid curves, and the numerical solution of the noisy Langevin equation in Eq. (88) shown with the noisy curves.

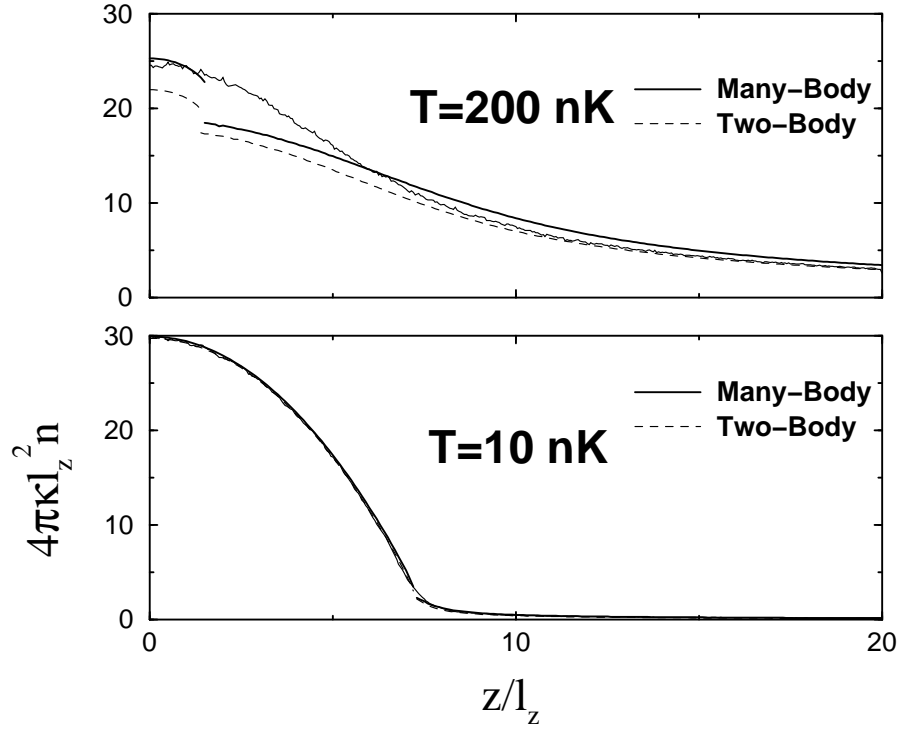


FIG. 11. Study of the many-body renormalization effects on the density profiles. The exact results are also shown with the noisy curves.

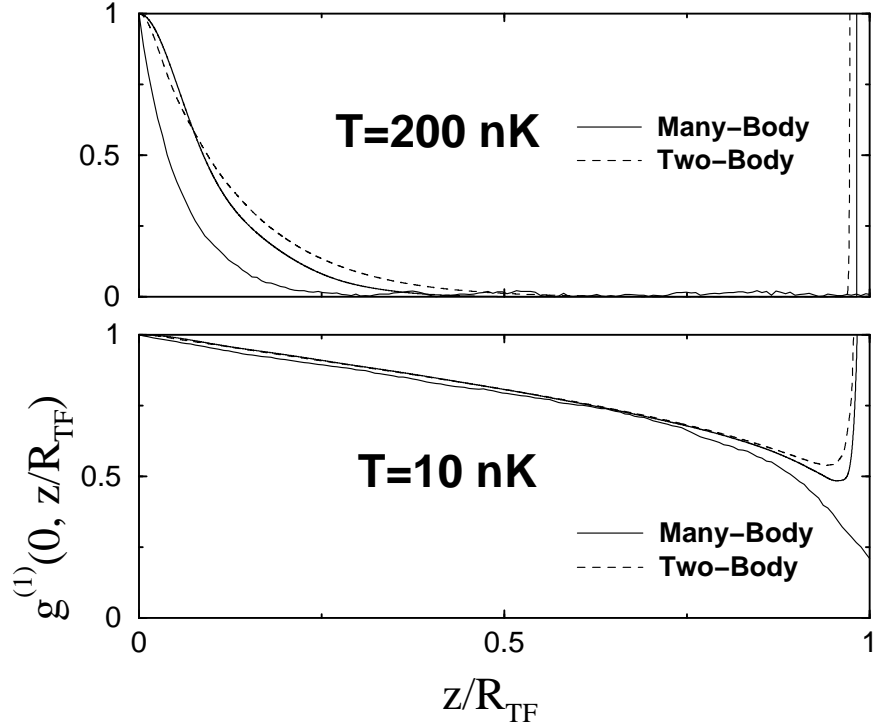


FIG. 12. Study of the many-body renormalization effects on the phase correlation function. The exact results are also shown with the noisy curves.

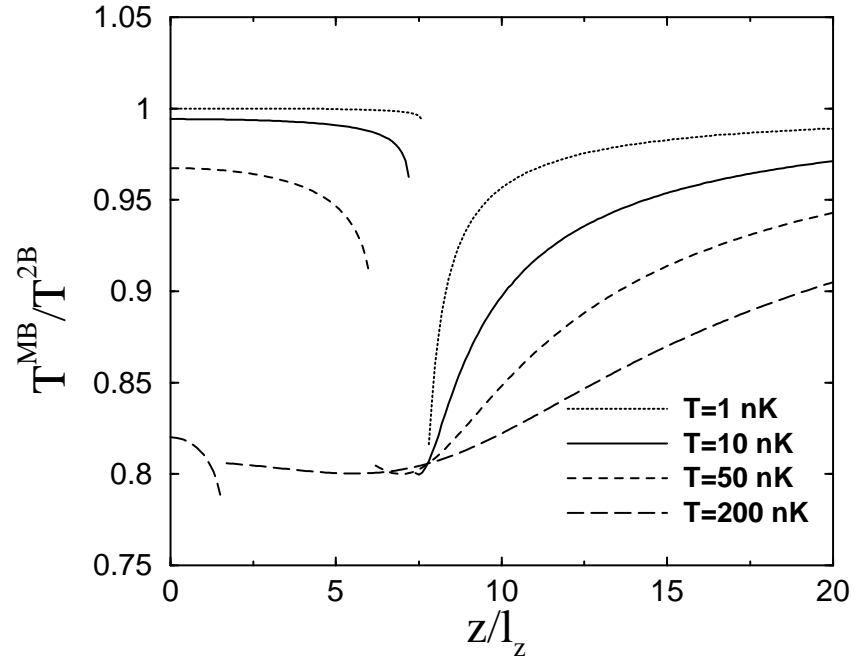


FIG. 13. The many-body T-matrix T^{MB} as a function of the distance from the center of the trap, for four different temperatures.